

Mind the Gap: From Resolving Theoretical Foundations of Chiral(ity)-Induced Spin Selectivity to Pioneering Implementations in Quantum Sensing

Yan Xi Foo^{1,2}, Aisha Kermiche², Farhan T. Chowdhury^{3,4,2}, Clarice D. Aiello^{2,5} and Luke D. Smith^{3,4}

¹⁾*Quantum Science and Engineering Centre (QSec), Nanyang Technological University, SG 639798, Singapore*

²⁾*Samueli School of Engineering, University of California, Los Angeles, CA 90095, USA*

³⁾*Department of Physics, University of Exeter, Stocker Road, Exeter, Devon, EX4 4QL, United Kingdom.*

⁴⁾*Living Systems Institute, University of Exeter, Stocker Road, Exeter, Devon, EX4 4QD, United Kingdom.*

⁵⁾*Quantum Biology Tech (QuBiT) Lab, Los Angeles, CA 90095, USA*

(Dated: 12 August 2025)

The chiral(ity)-induced spin selectivity (CISS) effect, where electrons passing through a chiral medium acquire significant spin-polarization at ambient temperatures, has been widely observed experimentally, yet its theoretical foundations remain actively debated. Open questions persist regarding whether CISS originates from helical geometry or more general chirality, and whether a unified mechanism can account for phenomena across solid-state and soft-matter systems, mesoscopic films, and single molecules. Clarifying the interrelations between existing models is essential to determine if a universal picture of CISS can be found or whether system-specific models are required, and if so, where their common starting point should lie for a workable classification of CISS manifestations. Despite this theoretical fragmentation, recent studies of CISS effects in electron transfer systems, magnetic field sensitivity and coherence of radical pair reactions, polarized electroluminescence in chiral hybrid perovskites, DNA-based biosensors, and enantioselective detection, highlight its broad conceptual relevance and potential applications in spintronics, molecular sensors, and quantum information processing. In this review, we help bridge the gap between theory, experiment, and implementation, with a particular focus on prospects for quantum sensing and metrology. We outline fundamental frameworks of CISS, clarifying what constitutes the ‘chiral’, the ‘induced’, and the ‘spin-selectivity’ that makes up CISS, before going on to survey key model realizations and their assumptions. We examine some of the emerging quantum sensing applications and assess the model-specific implications, in particular exemplifying these in the context of spin-correlated radical pairs, which offer a promising, tunable, and biomimetic platform for emerging molecular quantum technologies.

I. INTRODUCTION: ON CHIRALITY AND CHIRAL(ITY)-INDUCED SPIN SELECTIVITY

The notion of chirality stems from fundamental concepts in geometry. Roughly, an object is chiral if it breaks mirror symmetries along any plane of reflection. In high-energy physics, the Wu experiment famously demonstrated β -decay to be spin-selective and chiral (in Poincare transformations), establishing how the weak interaction violates parity¹. Chirality has since come to play a pivotal role across scientific disciplines, for instance in biochemistry—where enantiomers (i.e. chiral images) of the same compounds, that otherwise ought to be chemically identical, can exhibit significant pharmacological differences due to differing chirality^{2,3}. By definition, chiral biomolecules can exist in all their enantiomeric configurations; yet in-vivo, all genetic polymers (DNA/RNA, and their composite residues) exclusively exist in their right-handed enantiomeric forms, while all amino acids are found in the left-handed form. This gives rise to the emergence of self-assembling chiral structures on a macromolecular and cellular scale⁴. Thus, chirality arguably arises as a defining feature of life itself, with living systems by and large exhibiting almost perfect homochirality despite the significant entropic

costs entailed^{5–7} (for interesting exceptions, see a review on chirality and extraterrestrial life by Glavin *et al.*⁸). While such asymmetry strongly suggests that chirality plays a pivotal role in regulating biochemical processes, the precise mechanisms by which it does so remains a long-standing scientific mystery^{7,9}. A prominent candidate to address this gap in our understanding is the phenomenon of chiral(ity)-induced spin-selectivity (CISS), which broadly encompasses how electrons passing through a chiral (and often helical) medium acquire spin-polarization, and other anomalous spin dynamics^{10–16}.

The CISS effect was first observed, and the term introduced, by Ray *et al.* in 1999¹⁷, when spin-polarized photoelectrons ejected from thin chiral biomolecular films adsorbed onto an Au interface displayed asymmetric scattering $\sim 10^3$ larger than those reported in chiral gas-phase studies^{18,19}, suggesting for the first time a connection between helical geometry and quantized spin angular momentum. Subsequent studies on biomolecules have observed CISS to be optimized at room temperatures^{20,21}, thus raising exciting possibilities for designing robust chiral(ity)-based quantum devices, and spintronic applications, operating at ambient conditions. Experimental studies of CISS, seeking to uncover its fundamental

underpinning mechanisms, have since flourished into a dynamic and multifaceted field. It has furthermore emerged as a spin-manipulating paradigm underpinning an opportunity for designing controllable and precise quantum sensors^{22–28}. Overall, the key experimental realisations of CISS can be broadly partitioned into four broad categories:

1. **Spin-to-charge conversion through metal-to-chiral-medium junctions**, including microscopic studies of driven electron transport through chiral biomolecular nanojunctions^{29–31}, quantum Hall-response & induced magnetic order of metal interfaces with adsorption of chiral monolayer^{32–36}.
2. **Photoexcitation of chiral molecules**, in particular photoemission spectroscopy and Mott polarimetry of chiral monolayer absorbed onto metal substrate^{17,37,38}.
3. **Interface-less biochemical processes**, including intersystem crossing dynamics & radical pair formation in donor-chiral bridge-acceptor enantiomers³⁹, and arguably chiral transmission^{40,41}.
4. **Application-driven and biomimetic device development**, which seeks to harness the robustness of CISS at ambient temperatures. These include emerging technologies for efficient enantiomeric separation^{42–44}, oxygen-evolution^{45,46}, molecular machines⁴⁷, molecular qubits²², spin-optoelectronics^{48–52}, quantum-assisted magnetic sensing^{53–55}, and prospectively room-temperature qudits²⁶.

While the above does not serve as an exhaustive overview, it lays out broadly illustrative examples on the state of the field, which has covered wide ground since its inception. This diversity of experiments, though telling of the universality of CISS, has also contributed to a highly-fragmented picture of CISS characteristics. What often emerges is a set of structure-property/function relationships (Fig. 1), that are not directly comparable across experiment classes⁵⁶. This intriguing breadth of findings calls for theoretical efforts to better account for and predict CISS properties. To this end, a spin-momentum locking picture is often employed, proposing spin-orbit coupling (SOC) to be the defining component in CISS. In this framework, SOC couples the linear momentum of an electron to its spin angular momentum, resulting in electron motion being energetically favorable when they are parallel or antiparallel, depending on the handedness of the helical medium (Fig. 2).

A SOC mediated mechanism alone, however, cannot account for the spin-selectivity magnitudes observed in experiments^{57–60}, which becomes apparent from an elementary order-of-magnitude²⁶ estimation. Consider the rest-frame of an electron in motion along a helical path with some incident electric field, \mathbf{E}_{ext} : the electron incurs an effective magnetic field due to the field, $\mathbf{B}_{\text{eff}} = -c^{-2}\vec{v} \times \mathbf{E}_{\text{ext}}$, while possessing a magnetic moment, $\vec{\mu} = -g_s\mu_B\hbar^{-1}\vec{\sigma}$. The effective magnetic field exerts a torque on the magnetic moment, resulting in a Larmor interaction energy that is equivalent to a Rashba-like spin-orbit coupling: $\Delta H_{\text{SO}} = -\vec{\mu} \cdot \mathbf{B}_{\text{eff}} = \lambda\hat{n} \cdot (\vec{\sigma} \times \vec{p})$. By

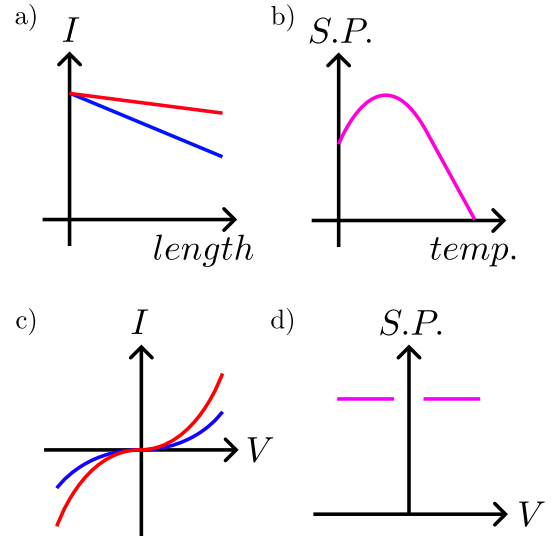


FIG. 1. Example graphs for structure-property relations used to characterize CISS at steady-state for spin-valve-like setups in which an organic chiral molecule or self-assembled monolayer acts as the spacer: the blue and red lines represent opposite magnetization of the spin-analyzer (for example, an atomic-force-microscopy tip); (a) charge current may decrease at a higher rate with respect to length of the chiral layer when setup magnetization is unfavorable to majority spins under transport; (b) spin-polarization as indexed by magnetocurrent anisotropy may peak at near-ambient temperatures; (c) charge current-potential difference graphs may suggest nonlinear-response and point to charging effects or the dielectric behavior of the chiral organic layer being strong; (d) spin-polarization may be relatively constant with regards to bias voltage, save for an undervolted regime (in which too little current passes for reliable measurement) and an overvolted regime.

this account, spin-degeneracy is broken and an energy gap opens. Assuming Boltzmann statistics, the energy gap for this spin-splitting gives rise to a population ratio to the factor of $\exp(-2\Delta H_{\text{SO}}/k_B T)$. Supposing one expects to retrieve a 20% population ratio at ambient temperatures (~ 300 K), this requires an expected spin-splitting field strength of ~ 20 meV, which is a magnitude apart from expected SOC fields of bare hydrocarbons. Much activity in CISS theory has since been devoted to accounting for the anomalous spin-polarization strengths observed. Concurrently, models attributing CISS's strength to rich nonequilibrium interfacial effects have also been proposed, from interface-orbital magnetization^{61,62} to spin-blockade & charge-displacement mechanisms^{15,57}, collectively giving rise to a more comprehensive theoretical treatment of CISS in nanojunctions.

It is increasingly evident that CISS should not be treated as a single, homogeneous phenomenon, but rather as a set of related effects that manifest differently depending on the experimental context. Each regime—be it solid-state transport, soft-matter photophysics, or biochemical electron transfer—possesses its own assumptions and constraints, requiring tailored theoretical approaches. However, this fragmentation has in turn given rise to a vast array of frameworks that preclude

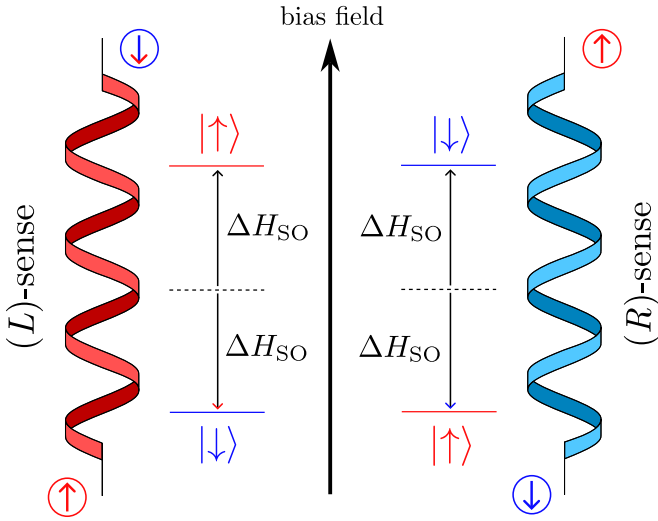


FIG. 2. Schematic diagram of the naive CISS mechanism. Electrons moving along a helical potential will experience an effective magnetic field that interacts with the electrons' spin in a manner such that opposite spin-orientations will prefer to travel in opposite directions. This spin-preference flips when the helical-configuration is reversed from left-handed to right-handed and vice-versa.

inter-applicability. Given the diversity of materials and platforms in which CISS finds itself relevant, a fundamental question is raised: What lies at the core of CISS? It is our view that, contrary to the perceptible fragmentation in the theoretical literature, a coherent and unifying understanding can nevertheless be gleaned. In this review we proceed by first laying out brief summaries of core mechanisms proposed to underlie CISS. Next, we consolidate developments in the theoretical literature in a systematic manner to give a brief overview of the trends thus far and highlight future directions. We conclude with a discussion of CISS's technological potential in the context of quantum sensing. We note that this review is not intended as a comprehensive survey of the CISS literature—broader accounts can be found elsewhere⁶³—but instead we focus on discerning common identifiable conceptual threads across the diverse manifestations of CISS, the emergence of distinct mechanisms in specific experimental realizations, and the implications these have for emerging quantum metrology applications^{22,64,65}. We hope this contribution will assist in demystifying CISS and underscore its potential to be primed for near-term applications in spintronics, biochemical industrial application and the quantum information sciences⁶⁶.

II. HOW DOES SPIN SELECTION IN CISS OCCUR?

Although CISS is conceptually underpinned by spin-transfer, to our knowledge there currently exists no apparatus that can directly measure spin-currents. Observation of CISS thus necessarily relies on spin-to-charge-current conversion and must draw from more indirect signatures. Benchmarking of CISS is further compounded in difficulty by the soft-matter and dielectric properties of biomolecular thin films giving rise

to potentially inconsistent structure-function properties of unclear origin, most exemplified by the temperature-dependence of CISS^{20,21,67,68}. A more thoroughgoing review of the experimental landscape and the many ways CISS has been indexed can be found in Bloom *et al.*'s extensive review⁶³. Theoretical investigations in CISS-junction transport have in turn been split between using either spin-transmission probabilities or charge-current values as a measure of spin-polarization, which are not equivalent nor necessarily related quantities⁶⁹. Additionally, the notion that spin-selectivity alone is being measured is called into question by Liu *et al.*⁷⁰, who notes that spin no longer provides a good quantum number due to SOC; CISS rather selects via the total electronic angular momentum quantum number ($j = s + l$), suggesting potential for orbitronics applications. This mix of analyses brings to the fore the proverbial elephant-in-the-room: how does spin-selection in CISS precisely occur, and how should experimental signals be understood in the context of proposed mechanisms? In the subsections to follow, we sequentially cover the questions: What is spin-selectivity? How is it induced? And what falls within the purview of 'chirality' in CISS?

A. Does Spin-Orbit Coupling Alone Give Rise To Spin-Selectivity?

Insofar as SOC is pivotal to CISS, the question of how SOC affects spin-selection is seldom addressed as compared to how SOC may have been enhanced in CISS to close the strength-gap. The spin-momentum locking picture posits simply that electrons with unfavorable spin-states relative to their motion will back-scatter, but by what means will this back-scattering occur? Indeed, Bardarson's theorem, which follows on from Kramer's degeneracy, implies that for time-reversal symmetric non-dissipative spin-1/2 systems, the transmission eigenvalues of both spin-configurations should be equal (i.e. spin-polarization should be forbidden in two-terminal junctions)⁷¹; its implications for CISS have been a chief subject of exploration by Utsumi, Aharonov, & Entin-Wohlman^{12,72,73}.

How, then, can we reconcile the above mentioned fundamental symmetry constraint with the experimentally observed spin selectivity in chiral systems? Let us first examine the equilibrium case in which no external bias is applied onto our system. We start by detailing a more commonly-encountered perspective from spintronics: spin-orbit coupling gives rise to spin-momentum locking, which can arise in spin-polarized currents. Considering a single-channel model, a Rashba-like spinor Hamiltonian for a quantum wire can phenomenologically describe the essential physics of our system, which can be denoted in reciprocal-space by:

$$\hat{H}(k) = -2t\sigma_0 \cos k + 2\alpha\sigma_z \sin k - h\sigma_x \quad (1)$$

where $t, \alpha, h \in \mathbb{R}$, while $\{\sigma\}$ denote standard Pauli matrices.

Visualising the spin-state energy bands in Fig. 3, finite α describes SOC effects and results in the splitting of the spin energy-bands (note that these are not spin-polarized); and a further non-zero h denotes spin-spin correlations or quasi-

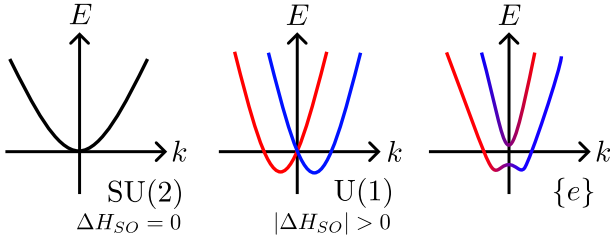


FIG. 3. Dispersion relations for 1D Rashba-like Hamiltonian. The spin energy-bands are degenerate before the introduction of SOC (left). At weak SOC strengths, the bands split (middle) while spin-spin correlations give rise to an avoided crossing (right), describing how spin-momentum locking occurs. Notably, one expects the electronic ground-state to have non-zero crystal-momentum and non-zero spin angular-momentum.

Zeeman effects that mix the spin-bands and gives rise to avoided crossings. Here, it is apparent that SOC lifts spin-degeneracy (specifically breaking SU(2) symmetry) and gives rise to spin-momentum locking. Intuitively, one would expect that the helical geometry *intrinsically* gives rise to a finite spin-current. And yet, it would appear that such an expected spin-current is not sufficient in arriving at an asymmetric spin-accumulation. We can consider an ideal scenario of CISS ex-

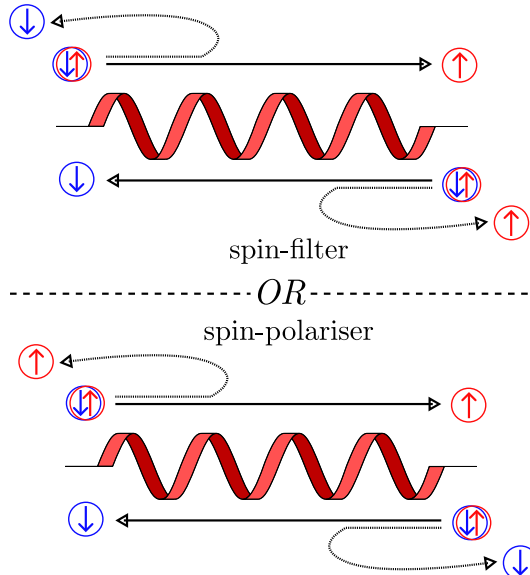


FIG. 4. Schematic diagrams of spin-filter (top) and spin-polarizer (bottom) pictures. In the spin-filter picture, spin-momentum locking results in spin-dependent transport such that opposite-valued spins are preferentially transmitted in opposite directions. Spinful particles travelling in unfavorable directions are reflected. In the spin-polarizer picture, reflected particles necessarily undergo a spin-flip since no dissipative spin transport can occur at equilibrium.

hibiting dissipationless coherent/ballistic transport with unpolarized sources. In the absence of an external applied magnetic field, time-reversal symmetry (of the Hamiltonian) is preserved; Wolf *et al.*⁷⁴ points out that no equilibrium spin transport or accumulation can arise accordingly, since equi-

librium dictates the scattering-matrix relations:

$$\sigma_r + \sigma_{r'} = 0 \quad ; \quad \sigma_{r'} + \sigma_t = 0, \quad (2)$$

in which $\sigma_{r(t)}$ denotes the spin expectation-value for the reflected(transmitted) wave, while primed variables correspond to those of an incident wave entering from the opposite end.

Given $\sigma_t = -\sigma_{t'}$, for injected spin currents, back-scattered electrons must have the same spin as transmitted ones:

$$\sigma_r = \sigma_t = -\sigma_{r'} = -\sigma_{t'}. \quad (3)$$

In other words, reflected waves and transmitted waves incident from opposite directions, hence travelling in the same direction, hold opposite spin-states (Fig. 4), a conclusion previously corroborated by a scattering-matrix analysis from Utsumi *et al.*⁷³. Additionally, we may argue for this on *ad absurdum* grounds: under the spin-momentum locking picture, a lone helical molecule at finite temperature would undergo spin-accumulation on its ends by itself owing to Brownian electron motion at equilibrium and become fully self-polarized barring any relaxation mechanisms; so all coiled wires would be spin-polarized by default. But this alone does not suggest a physical basis as to how such spin-selection may arise. Yang *et al.*^{75,76} proposes along similar symmetry grounds that a spin-flip reflection must be inherent to CISS; but assuming ballistic or dissipationless travel, no scattering events in general can occur within the CISS molecule to give rise to such a spin-flip. One possible resolution to this is interfacial: the CISS-junction itself acts as a scatterer that induces spin-flip scattering prior to entry. Previous spin-active tunnelling studies^{77,78} have proposed that the helical shape of the junction generates a curvature-induced quantum geometric potential that causes spin-flips.

Alternatively, minimal models recast the CISS-junction as a scattering region with an anisotropic dipole field⁷⁹ or treat the SOC as a barrier potential varying with direction as studied by Varela *et al.*⁷⁷ as illustrated in Fig. 5, though it has been noted that the latter effort does not confer spin-selectivity as-is⁸⁰. Additionally, we may extend from the equilibrium regime into the transport regime and view CISS as a form of current-induced spin-polarization. Suppose one subjects a linear electric bias onto a Fermi distribution of electrons within such a picture (i.e. $\exists E \Rightarrow f_k \rightarrow f_k^0 + \delta f_k$). This gives rise to a non-equilibrium steady state in which the spin states are split, giving rise to a spin-asymmetry describable as:

$$\delta s = \sum_k \langle S \rangle_k \delta f_k, \quad (4)$$

where $\langle S \rangle_k$ denotes the expectation value of spin for the k -th mode. Invoking the Boltzmann approximation, we can recast the spin current as a spin-wave:

$$\delta s = \sum_k \langle S \rangle_k \gamma_k (v_k \cdot E) \frac{\partial f_k}{\partial E}, \quad (5)$$

where γ indicates the gamma distribution, and v the spin-wave group velocity. The electric bias also generates a charge cur-

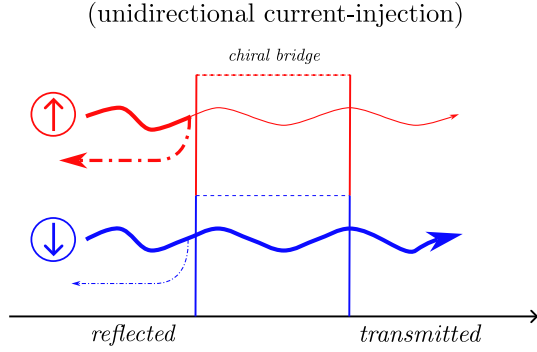


FIG. 5. Illustration of CISS as a barrier potential, showing unidirectional charge current. As an example, spin-up particles have to tunnel through a larger barrier and are thus preferentially reflected. In the equilibrium case, when bidirectional current is considered, this will result in zero spin transport and accumulation. Thus, the ‘inherent spin-flip’ necessary for the spin-polarizer picture can be construed as an interfacial effect.

rent given by:

$$j = \frac{e}{V} \sum_k v_k \delta f_k, \quad (6)$$

and as such, so long as the spin expectation-value is non-zero for some k , it would seem that a charge current is naturally accompanied by a finite spin current. However, is such spin current tantamount to spin-transport or spin-accumulation? Even in the transport regime, it can be shown that such a shifting of the Fermi sea is not equivalent to *preferential transmission of spin-species*.

We can call upon a physical argument by taking a gauge-covariant formulation of the Hamiltonian with SOC and obtaining its effective electromagnetic fields, an approach initially offered by Fröhlich & Studer⁸¹ and Tokatly⁸². Consider first the generic Pauli-Schrödinger Hamiltonian for a lone electron in an external scalar potential Φ and vector potential \mathcal{A} , with corrections up to c^2 (derivable from performing the Foldy-Wouthuysen transformation onto the Dirac Hamiltonian):

$$\begin{aligned} H = & \frac{\mathbf{\Pi}^2}{2m_0} + m_0 c^2 - e\Phi + \frac{e\hbar}{2m_0 c} \mathbf{B} \cdot \boldsymbol{\sigma} + \frac{e\hbar}{8m_0^2 c^2} \operatorname{div} \mathbf{E} \\ & + \frac{e\hbar}{8m_0^2 c^2} [\mathbf{\Pi} \cdot (\boldsymbol{\sigma} \times \mathbf{E}) + (\boldsymbol{\sigma} \times \mathbf{E}) \cdot \mathbf{\Pi}], \end{aligned} \quad (7)$$

in which $\mathbf{E} = -\nabla\Phi - (1/c)\partial_t \mathcal{A}$ is the electric field experienced, $\mathbf{B} = \operatorname{curl} \mathcal{A}$ is the magnetic field experienced, $\mathbf{\Pi}$ is the canonical momentum, defined by $\mathbf{\Pi} = -i\hbar\nabla + (e/c)\mathcal{A}$. In order of appearance, the Hamiltonian includes contributions from the electron’s kinetic energy, its rest mass, potential energy due to $\mathbf{\Pi}$, the Zeeman term, the Darwin term, and lastly the spin-orbit coupling term.

The Pauli equation hosts a U(1) \times SU(2) symmetry group; since the electromagnetic U(1) gauge field and the isospin SU(2) gauge fields commute, we may safely focus only on

how SU(2) transforms. Using Einstein summation convention, let us define \mathcal{A}_μ ($\mu \in 0, x, y, z$) as the non-Abelian SU(2) vector potential such that its components are given by:

$$\mathcal{A}_0 = -\frac{e\hbar}{m_0 c} B^\nu \tau^\nu; \quad \nu \in [x, y, z], \quad (8)$$

$$\mathcal{A}_i = -\frac{e\hbar}{m_0 c^2} \epsilon_{ij\nu} E^j \tau^\nu; \quad i, j \in [x, y, z], \quad (9)$$

where ϵ is the Levi-Civita symbol and $\tau^\nu = \sigma^\nu/2$ are the generators of SU(2) in the fundamental representation (i.e. normalised Pauli matrices). By Noether’s theorem, the gauge invariance of our Hamiltonian implies the existence of a covariantly conserved current, ξ , governed by:

$$D_\mu \xi_\mu = 0, \quad (10)$$

where D_μ represents the covariant derivative set as $D_\mu = \partial_\mu - i\mathcal{A}_\mu$. The definition of covariant derivatives allows us to form a compact Euler-Lagrange equation after recasting the Hamiltonian operator as $i\partial_t$:

$$iD_0 \psi = -\frac{\hbar}{2m} \sum_i D_i D_i \psi, \quad (11)$$

where ψ is the fermionic field operator, $(\psi_\uparrow, \psi_\downarrow)$. This lends to a simple formulation of the action:

$$S = \int dt d\mathbf{r} i\psi^\dagger (D_0 \psi) - \frac{\hbar}{2m} \sum_i (D_i \psi)^\dagger (D_i \psi), \quad (12)$$

where we have implicitly evaluated the wavefunction in position space. Here, it can be shown that the action remains gauge-invariant under local transformation, definable as $\Psi \rightarrow U\Psi$, $\mathcal{A}_\mu \rightarrow U\mathcal{A}_\mu U^{-1} - i(\partial_\mu U)U^{-1}$, where $U = e^{i\theta^\alpha \tau^\alpha}$ is some arbitrary unitary SU(2) matrix. And taking the matrix decomposition, $\xi_i = \xi_i^\alpha \tau^\alpha$, such that $\xi_i^\alpha = \partial S / \partial A_i^\alpha$, the form of the Noether current can thus be written out as:

$$\xi_0^\alpha = \psi^\dagger \tau^\alpha \psi = s^\alpha, \quad (13)$$

$$\xi_i^\alpha = -\frac{i}{2m} [\psi^\dagger \tau^\alpha (D_i \psi) - (D_i \psi)^\dagger \tau^\alpha \psi] - \frac{1}{4m} A_i^\alpha \hat{n}, \quad (14)$$

where \hat{n} is the unit-vector in the i -direction. We see explicitly that ξ_0 corresponds to the spin density; accordingly, ξ_i returns the spatial spin-current we are after.

The above also leaves us with the continuity equation:

$$\partial_t \xi_\mu^\alpha + \epsilon_{\alpha\beta\eta} A_\mu^\beta \xi_\mu^\eta = 0, \quad (15)$$

in which the second term encodes the chiral anomaly via spin precession in a magnetic field for $\mu = 0$, and otherwise an “internal spin torque”⁸² for $\mu = x, y, z$. As the current form of the spin current can be cumbersome, one can instead derive the SU(2) effective field tensor:

$$F_{ij} = \partial_i A_j - \partial_j A_i - i[A_i, A_j], \quad (16)$$

Here, $j = 0$ gives the dissipative electric-like part of the field while $j = x, y, z$ gives the nondissipative magnetic-like part

of the field. The effective magnetic field gives rise to non-dissipative equilibrium spin currents and hence do not contribute to spin accumulation⁸³; contributions to spin accumulation must arise from the dissipative effective electric field.

If no external magnetic field is applied, then F_{i0} is reduced simply to $-\partial_i A_i$. Supposing a simplified CISS model in which transport is set in the z -direction, we may ignore F_{x0} , F_{y0} and we assume that only $\partial_i E_z$ is negligible, giving:

$$F_{z0} = \frac{e\hbar}{m_0 c^2} \partial_t (E^x \tau^y - E^y \tau^x). \quad (17)$$

In other words, spin-up and spin-down states experience the same dissipative field strength up to a phase difference.

On the contrary, the non-Abelian effective magnetic fields (such as $F_{xy} = \frac{e\hbar}{m_0 c^2} (|E^x| - |E^y|) \tau^z$) may display unequal field strengths between the spinor states. This generates a spin current that is non-dissipative and hence does not contribute in scattering-matrix analyses. Unlike charge currents, non-dissipative spin current can still persist due to the chiral anomaly even if no dissipative spin current can be drawn, and this can result in a magnetic order or spin-texture when coupled with spin-momentum locking, such that biomolecular CISS under bias effectively gives rise to soft matter ferromagnets. Such magnetisation is linked to spontaneous time-reversal symmetry breaking, and is not to be identified with explicit breaking of time-reversal symmetry at the level of the Hamiltonian, which remains invariant⁸⁴. It is thus difficult to take spin-selectivity as an intrinsic consequence of helical geometry. If the spin-filter picture is to be applicable, CISS should rather arise from scattering and external dissipative factors^{85,86}, interfacial effects, and charge-trapping⁸⁷ etc. as will be discussed in Sec. III E.

Non-dissipative and/or pure spin-currents may be simply probed by spin-to-charge conversion using the inverse spin-Hall effect, the Hanle effect, or by way of time-resolved Kerr microscopy, as demonstrated by Sun *et al.* who showcase CISS giving rise to highly anisotropic nonlocal Gilbert damping⁸⁸. However, as experimental setups often stage chiral molecules/molecular layers either in contact with magnetised materials or within external magnetic fields, CISS is commonly observed in inherently non-equilibrium conditions which the idealised scenarios described in this sub-section may be far removed from. Such insight is nevertheless essential to understanding the phenomenon and the directions future applications may take; we leave discussion of this rich topic for last in Sec. IV.

B. Onsager's Relations: Linear or Non-linear? Molecular vs Interfacial Mechanisms?

A persistent question in the CISS corpus is whether anomalous spin-selectivity strengths as reported in experiments originate intrinsically from SOC or whether these are enhanced by medium-specific processes. In other words, can CISS exist as a linear-response phenomenon? Briefly, given an out-of-equilibrium system in the linear regime, for which the coupled

flux-force transport equations are $J_j = \sum_k L_{jk} F_k$ with fluxes J_j and generalised forces F_k , Onsager's reciprocal relations state that the kinetic coefficients L_{jk} obey $L_{jk} = L_{kj}$ (i.e. they form a symmetric matrix). These relations reflect how microscopic time-reversal symmetry affects macroscopic dynamics, and generally no longer holds when time-reversal symmetry is broken. Accounting for applied fields B_m that break time-reversal leads to the generalised Onsager-Casimir relations, $L_{jk}(B_m) = L_{kj}(B_m)$. In the context of two-terminal CISS spin-valve-like set-ups, this means that the charge-conductance measured remains invariant under a reversal of magnetisation (for all magnetised components) and applied magnetic field if present: $G_{ij}(H, M) = G_{ij}(-H, -M)$. The direct implication is that there should be no anisotropy readings for CISS in the linear regime. Since CISS spin-valve experiments clearly do feature magnetocurrent anisotropy, one may conclude that biomolecular-CISS transport observations are inherently nonlinear whenever such setups do not feature the application of an external magnetic field onto target CISS molecules. This also raises the pertinent question: if SOC is not giving rise to both spin-polarization or conductance anisotropy, then what exactly is being captured in readings?

This line of thought has given rise to many coarse-grained theoretical analyses, elaborated further in Sec. III C, and it suggests that CISS's anomalous spin-selectivity levels in biomolecular setups may arise from experimental or material-dependent factors not fundamental to CISS (at ambient temperatures), lending well to explicitly nonlinear⁸⁹ or setup-dependent^{61,62} accounts. Notably, Dalum and Hedegård⁹⁰ argue that Onsager-Casimir reciprocity only holds in naïve conditions: spin-orbit coupling establishes a dipole moment across the molecule upon bias application, resulting in altered local-magnetisation for the leads at steady state. In this vein, Liu *et al.*⁹¹ observe a nontrivial linear contribution to magnetoconductance, attributable to the coercive field of the substrate (Ga,Mn)As giving rise to different conductance states when magnetisation is reversed. Such analyses highlight how the electronic/structural properties of all experimental components are susceptible to change upon bias, pointing towards

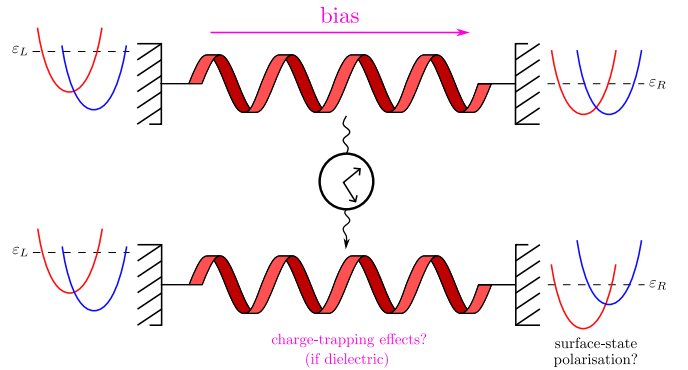


FIG. 6. Electric bias application across the biomolecular nanojunction can change the electronic properties of the setup-at-large, giving rise to surface-state polarization, charge-trapping, and other effects contributing to nonlinear-response.

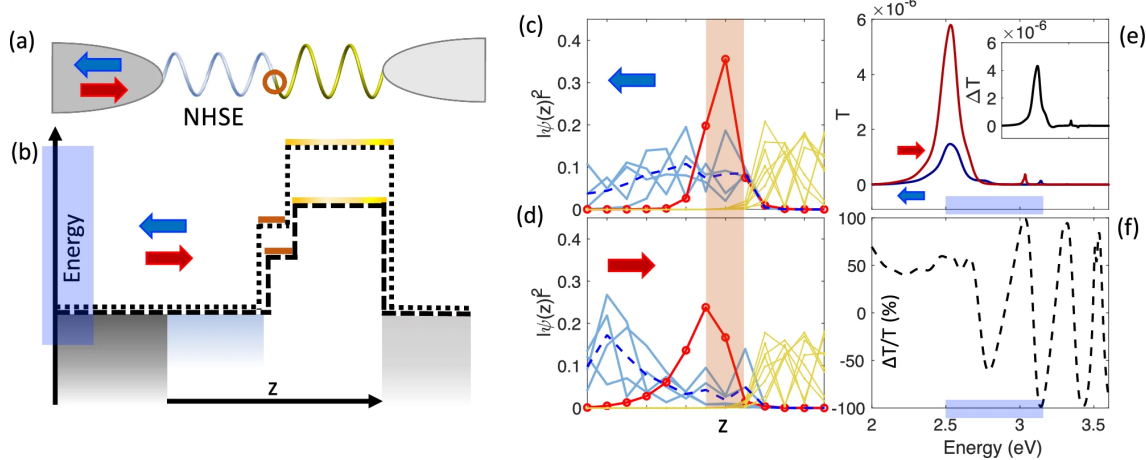


FIG. 7. Schematic of Zhao *et al.*'s charge-trapping model. (a) the non-Hermitian skin effect gives rise to localisation of interfacial wavefunctions, and interface-magnetisation augments their penetration into the chiral bridge. (b) Impurity/defect-sites act as charge-trapping centers. Localised impurity wavefunctions couple to interfacial wavefunctions, resulting in magnetisation-dependent barrier-potential adjustments, breaking Onsager-Casimir reciprocity and allowing finite anisotropy from the linear-response regime. (Nonlinear-response still dominates in this model due to conductance amplification from barrier-tunnelling.) Crucially, this differentiates biomolecular/semiconductor-CIIS from that in chiral metals; free of defect sites, the latter respect Onsager relations. (c) & (d) Wavefunction spread of the interface (blue), the impurity (red), and the molecular region past the impurity (yellow) across the model for opposing interfacial magnetisations. The red-barred region indicates the impurity-site. (e) & (f) Transmission probability readings against chemical potential for opposing interfacial magnetisations at zero-bias. Reproduced with permission from Zhao *et al.*⁸⁷, Nat. Commun. **16**, 37 (2025). Copyright 2025 Authors, licensed under a Creative Commons Attribution (CC BY) license.

the importance of nonlinear interactions and feedback between experimental components (see Fig. 6). A broader introduction to such proposed ‘pictures-in-motion’ is given in Sec. III E on semiclassical models.

Xiao *et al.*⁸⁷ elaborate on above by comparing CISS to electrical magnetochemical anisotropy (EMCA), in which an external magnetic field is applied to some chiral conductor; both exhibit non-linear response against a driving electric field and feature induced spin-accumulation in leads like Au. Yet, EMCA preserves Onsager-Casimir relations, leading the authors to propose that biomolecular-CIIS’s unique magneto-transport properties may arise from charge-trapping within the dielectric bridge. Recent follow-up work by Zhao *et al.*⁸⁷ develops this idea thoroughly, as outlined in Fig. 7: due to the non-Hermitian skin-effect, the wavefunction of the magnetised interface may be exponentially localised either towards the interface or spread further into the bridge, depending on magnetisation direction. This interfacial wavefunction couples with localised impurity/defect-sites in the bridge, and altering the wavefunction distribution also modifies the energy of localised impurity states (effectively, the barrier potential), thus changing the electronic properties of the set-up and circumventing the Onsager-Casimir relations *even at zero bias*.

Going beyond anisotropy readings, dominant linear-response in CISS has been amply observed on inorganic chiral media or chiral metals where Onsager-Casimir reciprocity is not expected to fail. (Of note, Yang & van Wees⁹³ suggest that alternative anisotropy measures may instead be used, such as changing the magnitude of magnetisation or a rotation of an applied magnetic field not amounting to reversal.)

Transport experiments have, for instance, been conducted without magnetic field application on disilicide crystals⁹⁴ and transition-metal dichalcogenide monolayers⁹⁵, all of which showcase linear current-to-voltage response, attributable to a strong Weyl-type SOC that, given $|\alpha_{(x,y)}| \ll \alpha_z$, results in an effective one-particle Hamiltonian:

$$H \cong \frac{\hbar^2 k_z^2}{2m} + \alpha^2 k_z \sigma_z \cong \frac{\hbar^2}{2m} \left(k_z \pm \frac{m\alpha_2}{\hbar^2} \right)^2, \quad (18)$$

which acts as a perturbation to the inversion-breaking crystal field that hybridises the Rashba bands, facilitating spin-momentum locking with monopole-like spin-texture. Most pertinent, however, are helical tellurium nanowires (geometrically akin to 3₁₀-helix peptides); they are naturally *p*-doped semiconductors and can be viewed as direct inorganic analogues of biomolecular junctions in CISS.

Recent work by Gupta & Droghetti⁹² employed ab-initio methods to show that for a bundle of tellurium nanowires bonded together by van der Waals forces, collinear magnetic moments emerge upon application of finite bias, spontaneously breaking time-reversal symmetry and giving rise to non-zero spin current in the direction parallel to charge transport within the linear-response regime (see Fig. 8). It should be noted that nevertheless the spin-resolved conductances remain the same, so their model does not act spin-selectively per se. In such uniform media, as Onsager-Casimir reciprocity remains upheld, magnetocurrent anisotropy becomes an ineffective index.

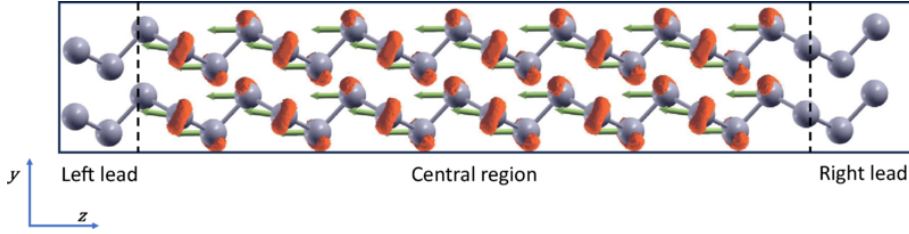


FIG. 8. Gupta & Droghetti's (2024) tellurium model schematic. The arrows represent the current-induced magnetic moments, and the orange regions mark the spin-z density isosurface. Time-reversal symmetry is spontaneously broken with bias application. Reprinted with permission from Gupta & Droghetti⁹², Physical Review B **109**, 155141 (2024). Copyright 2024 American Physical Society.

C. The Role of Symmetries: Chiral-Induced or Chirality-Induced?

The prototypical example of CISS occurs within a helical bridge, with non-trivial SOC arising chiefly from a helical geometry. Much of CISS studies revolve around helical structures or molecules. Geometric chirality, however, is broader than helical structures alone, and one example to counter narrow helical-centric interpretations of CISS are the prior-mentioned studies on inorganic chiral crystals, in which inherent chiral magnetic-order/spin-texture spontaneously breaks time-reversal symmetry (we refer to Cheong & Xu⁹⁶ for an overview). This begs the question, as outlined in Fig. 9: to what extent is CISS a point-chiral phenomenon as opposed to a helical or geometrically-chiral one?

The absence of chiral centres *per se* appears irrelevant to CISS insofar as they do not contribute to SOC. Mondal *et al.*⁴⁰ demonstrated how achiral monomers, when induced to self-assemble into helical macrostructures, produced opposite circular dichroism signals depending on the chirality of the initial solvent. An earlier work by Kulkarni *et al.*⁹⁷ provided evidence of the transport counterpart using magnetic-conductive AFM microscopy, showing that supramolecular helicity was sufficient for CISS. Given this, it is intriguing

to note that CISS is not limited to helical molecular structures but encompasses general structural chirality: Ghazaryan *et al.*⁷⁹ formulates CISS as a scattering phenomenon under second-order perturbation theory and casts the chiral bridge as an anisotropic dipole-field, retrieving spin-polarization while reproducing length- and energy-dependence trends. Such a dipole-centric perspective has been broached experimentally too, when Eckshtain-Levi *et al.*⁹⁸ observed via non-magnetic Hall measurements that cold-denaturation in alpha-helical oligopeptides can flip spin-polarization direction; simulations suggest that dipole-flips due to rearrangement of dipole-flips upon denaturation may be the underlying mechanism. Such dipole-centric models also implicitly account for charging of the molecular bridge by allowing for in-time non-equilibrium descriptions of CISS, which we discuss further in Sec. III E.

In light of both geometric- and point-chirality contributing to CISS despite the different analyses of their SOC-contributions (the former accountable purely from effective helical-motion, while the latter is better described as emergent from the configuration of σ - and π -type orbital overlaps), it is natural to probe at a higher level and question if chirality by itself can give rise to any relevant topological electronic properties⁹⁹ in CISS. At its simplest, we can map a 1D helix to a toy Su-Schrieffer-Heeger-like model by assuming continuous screw-sense symmetry and coherent transport. When the sites are arranged such that they admit a perfectly periodic unit-cell, the conservation of screw-sense helical momentum labels the model with a Zak phase upon the introduction of an external magnetic field (that breaks time-reversal symmetry), giving rise to a quantised charge-pump that carries no net spin; see Sacramento & Madeira's¹⁰⁰ study for a deeper investigation into the topological properties of such 1D chiral electronic chains. Any spin-selective effect that does not invoke an explicit magnetic field should therefore arise beyond the single Bloch-band description, for instance by employing multi-orbital frameworks to remain within the purely coherent paradigm as demonstrated by Utsumi *et al.*^{72,73}. Under the premise that a chiral biomolecule primarily functions as an *orbital-momentum* selector due to its weak SOC, Liu *et al.* go beyond a molecule-only picture and reveal the presence of a topological orbital texture via which orbital-polarisation is generated and then converted to spin-polarisation at the interface with a substrate of non-negligible SOC⁷⁰. However, the applicability of either coherent-transport approaches to explain experimental findings is uncertain: initial calculations

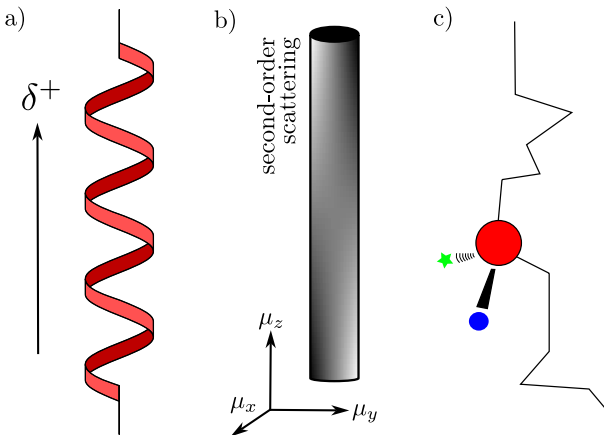


FIG. 9. Schematic depicting contexts where CISS can be considered: (a) a bridge with helical geometry; (b) a molecular wire equipped with an anisotropic dipole-field with no plainly structural chirality; (c) a molecule with point-chirality but no obvious emergent SOC.

by Gersten *et al.*¹⁰¹ and recently experimental investigations from Li *et al.*¹⁰² using both nonmagnetic and magnetic break-junction setups found that no significant dependence of magnetoconductance or I-V characteristics on enantiomeric handedness within the fully coherent transport regime, owing to interfacial SOC being too weak and transit time being too short for spin-filtering to occur at a coherent time-scale, accentuating the setup-dependent nature for the origin of the CISS effect.

More generally, in the absence of external magnetic fields and any crystalline structure, Weyl fermions with finite Chern number appear at time-reversal-invariant momenta for all symmorphic chiral space groups¹⁰³. Unlike Weyl fermions generated by band inversion, these chiral fermions exist *a priori* and their finite chiral charge implies that they can only be destroyed via pairwise annihilation, requiring application of a large magnetic field. Whether they manifest in chiral soft-matter is an intriguing avenue for further work, but it suffices to note at current that chirality is not a sufficient factor for spin-selectivity.

D. That Which We Call CISS: Open Questions and Avenues

What is CISS? The breadth of CISS belies the difficulty of building an overarching framework capable of encompassing all its realisations. On one hand, CISS occurs in deformable dielectric helical biomolecules/films in noisy ambient conditions, exhibiting nonlinear transport with strong substrate effects. On the other, CISS occurs in non-centrosymmetric crystalline structures and nanowires with none of the complications the former case brings. Both directions are equally rich with promise: the former explores spin effects in biology and the rise of biomimetic quantum/spintronics technologies, while the latter can open the door to unconventional superconductivity¹⁰⁴ and other magnetochiral effects. Controversy within the theoretical literature is symptomatic of this split in the field, and caution should be taken by new entrants therefore to ground their investigations in CISS within the assumptions of their respective fields. We argue that CISS can be briskly summarised under the following checklist:

1. Geometric inversion-symmetry breaking: A noncentrosymmetric structure or helical geometry gives rise to a spin-orbit coupling field.
2. Rashba-likeness: Such an intrinsic spin-orbit coupling field gives rise to a magnetic order, and thereby a spin-texture and spin current.
3. Selectivity: The presence of a spin current does not guarantee spin-selectivity or preferential transmission of spin-species; that lies in the purview of the retrieval or conversion mechanism within the physical setup.
4. Confounders/Enhancers: Electromagnetic properties of chiral object(s) can be altered by external setup components and vice-versa, potentially leading to anomalous effective SOC strengths and nonlinear response.

Beyond controversy in the traditional realisations of CISS-transport and CISS-transmission, novel observations on CISS have lead to surprising developments in both theory and application. One such example is the potential use of CISS for orbitronics or orbital-selectivity mechanisms^{35,70,74,105}, especially concerning media with negligible SOC. Additionally, non-adiabatic corrections for nonequilibrium nuclear motion can strongly affect reaction evolution and also transport characteristics in molecular junctions^{106,107}, leaving the extent of Berry effects in the neighborhood of (Kramers-)Weyl fermions an open question in CISS^{108,109}. And while the theoretical disagreements around CISS appear to arise largely from contextual differences, many open questions still remain as to the broader implications in emerging quantum engineering prospects for CISS. For example, do thermal fluctuations and phononic vibrations enhance or stymie CISS? Does CISS play a role in chiral transmission? Where does CISS fit into the broader realm of chiral phenomena from magnetic chirality to chiral quantum optics¹¹⁰? Most recently, Briggeman *et al.* exhibited analog simulation of 1D chiral molecular conductors by using AFM lithography to etch planar channels on an oxide-interface that explicitly break mirror symmetry in the electron potential landscape, thereby offering direct means to isolate purely geometrical chiral SOC effects¹⁰. In concluding this section, we hope that our discussion helps dispel some incertitude for those new to the area pertaining to the contentiously fractured state of the wider CISS literature, and we will now follow in the next section with a broad overview of theoretical efforts in CISS.

III. WITHIN THE GAP: MODELS, MECHANISMS, AND THE MISSING LINK

Having surveyed some foundational issues underpinning CISS theory, we now turn to organizing the key modeling approaches that have been advanced to explain the CISS effect within each broad class of experimental manifestations, running through excited-state frameworks to continuum models and tight-binding treatments before ending in spin chemistry and electron-transfer approaches to CISS. Through this, we hope to highlight the different regimes these separate modeling approaches cover, thus laying the conceptual ground to briefly discuss emerging applications, such as functional molecular devices, next-generation LEDs, plus quantum sensing and detection platforms, which we address in Sec. IV.

A. CISS in Excited-States: Theory behind Optical-Activity in Chiral Molecules under Photoexcitation

In Ray *et al.*'s¹⁷ initial paper, photoelectrons emitted from L-/R-stearoyl lysine biofilms exhibited asymmetric transmission using clockwise circularly-polarized light over its counter-clockwise counterpart, marking the first reported observation of CISS. Subsequently, Göhler *et al.*¹¹¹ found using Mott polarimetry that a chiral ds-DNA film bound to Au displayed spin polarization even with linearly-polarized light,

confirming chirality can by some mechanism induce spin-selectivity in transmission. But to what extent are these results attributable directly to transmission across the chiral film than they are indirectly to interfacial effects of chiral-film-adsorption upon the substrate? To better understand photoemission in CISS, it is useful to go over how natural optical activity arises in chiral bodies. This is well-covered by the theory of circular dichroism, in which the differential absorption of clockwise and counterclockwise circularly-polarized light is measured¹¹². Of note, a concise treatment for the lone electrically conducting helical-molecule case appears in Andrews & Tretton¹¹³, providing an intuitive classical analogy.

Heuristically, the rotating electric field of circularly-polarized light induces a static dipole moment along its direction of propagation, potentially altering electronic properties via mobile charge/spin-rearrangement and affecting the molecules' absorption spectrum; and the rotating magnetic field acts as an effective Zeeman-splitting field for electrons along the longitudinal (if perpendicular to the helical axis) or transversal (if parallel) directions, assuming the fields do not average to zero. However, gaseous/liquid-state chiral bodies (for which a lone-molecule approximation would be justified) are seldom used to probe CISS-transmission due to random dispersion/orientation of samples. Rather, CISS is tested on ferromagnetic substrates functionalised with organic chiral films. As such, photoelectrons are collected from both the chiral film and the substrate surface, with spin-polarization arising from both components and their interplay. Abendroth *et al.*³⁸, in an experimental study on the valence electronic structure of CISS-FM layers, propose that photoelectrons undergo spin-selectivity under three routes: firstly, scattering of FM surface electrons through the chiral fields (enhanced by proximity effects of the packed layer) experiences a lower work-function if the majority-spin state in the FM is also preferred by the chiral layer; secondly, incident photons can ionize adsorbed chiral-molecules given a high enough energy and emit photoelectrons from the chiral layer (thus forming a main source of spin-polarized photoemission differentiable between oppositely circularly-polarized light); thirdly, photoelectrons from the FM may collide with and ionise chiral molecules, resulting in secondary scattering processes; and fourthly, as the chiral layer builds up positive charge due to photoionisation, conduction electrons are induced to transfer into valence holes in the chiral layer, as seen in Fig. 10. This process is further compounded by spin-transfer torque effects when a magnetic order is induced in the substrate upon adsorption of a chiral layer³³.

B. CISS in Excited-States: Scattering Models for Photoexcitation

Given the complications as presented above, one prominent theoretical goal has been to find some analytical description that can capture the essential physics of CISS-transmission. A foundational effort is given by Yeganeh *et al.*¹¹⁴, in which scattering theory is used to model electron transmission through a helical potential dressed with a

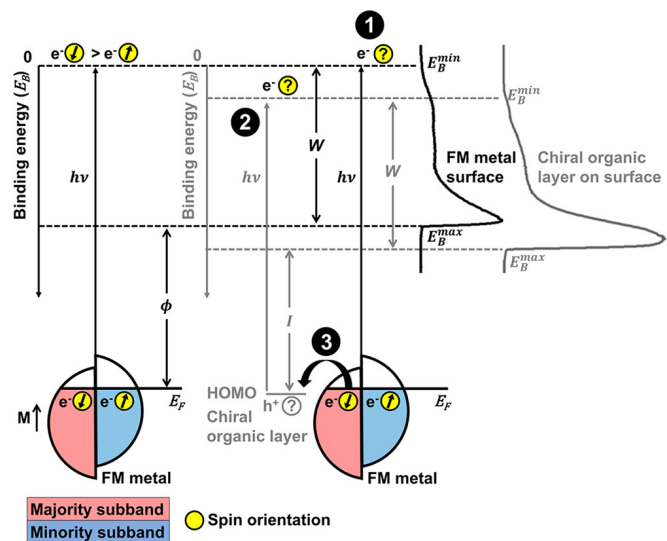


FIG. 10. Schematic by Abendroth *et al.* illustrating photoelectron spectroscopy on ferromagnet-substrate-chiral film setups and representative ultraviolet photoelectron spectra, annotated with routes to spin-selective emission: filtering of photoelectrons originating from the ferromagnet by the chiral thin-film (1), spin-polarized photoemission, indirectly influencing photoionisation energy (I) of the chiral-film (2), or filtering of conduction electrons supplied by the metal to fill holes left in the valence orbitals of the organic films, represented as highest-occupied molecular orbitals (HOMO) (3). In the case of linearly polarized light being incident on the setup, route (3) can still generate spin-selection. Reprinted with permission from Abendroth *et al.*³⁸, Journal of the American Chemical Society **141**, 3863-3874 (2019). Copyright 2019 American Chemical Society.

spin-orbit coupling field, assuming elastic first-order scattering. Their results yield that a finite pitch result in differential angular momentum transfer, validating chirality's role in spin-selectivity. However, asymmetry readings are too low to match experimental results, rendering chirality alone to be a necessary but insufficient factor. Subsequent work expands on this approach by considering the multiple-scattering regime¹¹⁵, interfacial conversion of orbital-to-spin angular momentum due to substrate SOC¹⁰¹, inelastic effects¹¹⁶, and a minimal model that generalizes the CISS-helix into a CISS-dipole⁷⁹. However, these analytic methods either do not give rise to anomalous spin-polarization readings as measured in Mott polarimetry, or cannot (in the case of interfacial effects) account for similar spin-polarization readings when substrates with low-SOC are used¹¹⁷. It stands to reason that either some non-equilibrium¹¹⁸ mechanism perturbs the set-up significantly that is not captured by the above methods, or there is some omitted factor in the chiral molecule itself that is responsible. Could there be more to the helical contribution to CISS than currently treated? We now move to discussing CISS-transport in waveguides in the next subsection, where we cover efforts to find some rigorous starting-point to study CISS.

C. CISS in Waveguides: Continuum Approximations and Geometric Efforts

That helicity itself is a main contributor to spin-selectivity is an attractive idea at first glance, but how exactly can helical contributions be quantified? A continuum formulation of CISS, though rarely featured in the literature, can serve as a robust starting-point to derive an effective low-dimensional Hamiltonian and recover geometric effects. One convenient method to study helicity is to employ a rotating Frenet-Serret frame, allowing the curved path to be parametrized by a single path variable while the curve's torsion and curvature then determine the frame's rotation. Infinite potential walls (implying adiabatic separation of tangential and transversal Hamiltonian components) can then be imposed along this path according to da Costa's thin-layer quantization method¹¹⁹.

As per da Costa, these non-inertial effects are captured via a 'geometric potential' that can be appended to the Pauli-Schrodinger Hamiltonian. Several early works¹²⁰ start from this point but do not explicitly investigate curvature-effects. Michaeli & Naaman⁷⁸ begin by considering a tubular waveguide rather than a quasi-1D wire, adding a strong dipole potential V_D growing linearly along the molecular axis. Likening CISS to a Klein-tunneling phenomenon, they describe their system with the Hamiltonian:

$$H_{N,l}(s) = E_N + V_D(s) + \frac{\mathbf{p}_s^2}{2m} + \frac{\mathbf{p}_s}{m} \cdot \hbar\gamma l + \kappa\vec{\sigma} \cdot \vec{L}_{\text{helix}} + \Delta E_l, \quad (19)$$

whose eigenstates are a product of two wavefunctions, one a harmonic oscillator in the plane perpendicular to the helical axis (s) and the other dependent on s , such that E_N refers to the energy level of the N -th state of the former, V_D the potential along s , the third-last term a centripetal-like potential, the second-last term SOC due to the confining helical potential, and the final term being a curvature-dependent energy-shift. And after applying the gauge transformation, $|\sigma_z^\pm\rangle \rightarrow \exp[\pm(i\pi s/R) \cdot |\sigma_z^\pm\rangle]$, they observe the emergence of a momentum-independent Zeeman-like component, κ/σ_y , from the rotating atomic SOC field. Here, the strong dipole component is proposed to extend CISS's energy range up to that of the dipole potential while enhancing spin-polarization by suppressing transmission of unfavorable spin-states, using Airy functions to model wavefunction decay. It should be duly noted that though the appearance of a Zeeman-like field brings about finite asymmetry in spin-transmission, this model does not break time-reversal symmetry at the Hamiltonian level. Geyer *et al.*¹²¹ then build on this work, investigating the validity of applying the thin-layer quantization method under a generic (scalar) SOC field. They demonstrate that the momentum-independent Zeeman-like term, given by $v\ell\vec{\sigma} \cdot \vec{B}$ in their derivation, arises from transversal degrees of freedom, originally omitted from Gutierrez *et al.*'s¹²⁰ treatment, preventing removal of SOC via gauge transformation.

However, these efforts take the Pauli-Schrodinger equation as their starting point which describe a Dirac fermion in an inertial frame, which the Frenet-Serret frames are not. Shitade & Minamitani¹⁶ attempt to circumvent this by employing

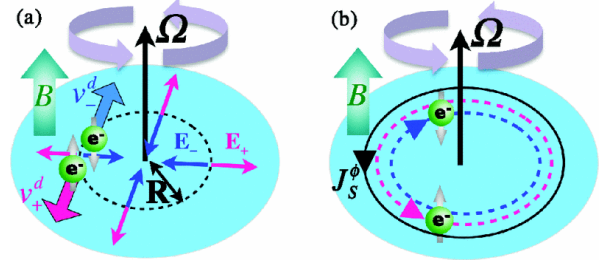


FIG. 11. Illustration by Matsuo *et al.* of their spin-mechatronics model. When a plane is made to rotate at some angular velocity and an external magnetic field is applied normal to the plane, opposite spins experience opposite effective effective fields, giving rise to opposite spin-currents. This can be interpreted as an inverse Einstein-de Haas effect. Reprinted with permission from Matsuo *et al.*¹²⁴, Physical Review B **84**, 104410 (2011). Copyright 2011 American Physical Society.

the generally-covariant Dirac equation, generating the Lagrangian directly from holonomic constraints to derive an appropriate single-electron Hamiltonian:

$$H = \frac{\mathbf{p}_s^2}{2m} + \frac{\hbar^2\kappa^2}{8m} + \frac{\hbar}{2} \cdot \frac{\{\mathbf{p}_s, \kappa\vec{\sigma} \cdot \vec{B}\}}{2}, \quad (20)$$

after applying the Foldy-Wouthuysen (non-relativistic) and the thin-layer approximations. Difficulty arises in this approach, however, as changing the order of approximations applied alters the form of the Hamiltonian, reflecting a necessity for further work into canonical quantization. Alternative curvature-focused continuum-model efforts that do not make use of thin-layer quantization do exist but are uncommon, like the scattering model of Medina *et al.*¹¹⁵, or Diaz *et al.*⁸⁹ where molecular deformation is accounted for by deriving an effective nonlinear model for electron transport¹²² through a helix composed of vibrating point dipoles, simplifying CISS to a Davydov-like model.

One conclusion common to efforts in this vein is that curvature-effects give rise to an effective momentum-independent Zeeman-splitting field. This appears to contradict Kramers' degeneracy, in which time-reversal symmetric systems should display equal transmission eigenvalues for both spin-configurations⁷¹. Furthermore, Gersten *et al.*¹⁰¹ demonstrated heuristically that on regular Cartesian coordinates, spin-flip contributions in the single-scattering regime and spin-precession throughout helical motion are both negligible, with spin-flip transition probability to order $\sim 10^{-9}$ and an estimated spin-rotation length-scale of $\sim 10^4$ relative to helical pitch. Such results are in line with Mashhoon's¹²³ spin-rotation coupling term, given by $\delta H_{SR} = \gamma(\delta H_{Thomas} - \Omega \cdot \mathbf{S})$, which is vanishingly small at below-relativistic speeds.

Though questions regarding quantization methods remain at-large, field-theoretic approaches may still be adopted. For instance, Matsuo *et al.*'s^{124,125} procedure to generalise the Pauli equation for non-inertial frames can be used to provide a rigorous background to Gersten *et al.*'s heuristics. Since Gersten *et al.* assume a constant z -velocity for the electron, we

can also model the electron as a particle on a rigid rotating rod on an inertial plane that is moving at some constant velocity in the z -axis with respect to an observer (Fig. 11). This allows us to study non-inertial effects of a particle on a constrained helical path in regular Cartesian coordinates, making it tractable to comparison while bypassing the quantization procedure, resulting in the single 2-spinor free Hamiltonian:

$$H = \frac{\vec{\pi}^2}{2m} + qA_0 + \mu_B \vec{\sigma} \cdot \vec{B} - \vec{\Omega} \cdot (\vec{r} \times \vec{\pi} + \frac{\hbar}{2} \vec{\sigma}) + \frac{\lambda}{2\hbar} \vec{\sigma} \cdot [\vec{\pi} \times q\vec{E}' - q\vec{E}' \times \vec{\pi}] - \frac{\lambda}{2} \text{div}[q\vec{E}'], \quad (21)$$

where the electric field is augmented as $\vec{E}' = \vec{E} + (\vec{\Omega} \times \vec{r}) \times \vec{B}$, accounting for a Lorentz boost due to an external magnetic field. Since SOC is to order m^{-2} while the spin-rotating term is to order m^{-1} , SOC contributions can be considered small in vacuum conditions; and in the absence of an external magnetic field, the spin-rotation coupling, $\vec{\Omega} \cdot \vec{\sigma}$, provides spin-splitting. Though this analysis corroborates the existence of geometric effects in CISS, their strength remains a matter of contention. On one hand, heuristically accounting for a linear electronic momentum of 1eV as with Gersten *et al.*¹⁰¹ makes such effects negligible. On the other hand, recent work from Bradbury *et al.*¹¹ account for non-Born-Oppenheimer effects using a phase-space formulation of electronic structure, predicting a strong spin-Coriolis effect even for electrons of small molecules. And while there are innovative schemes to explicitly test curvature-dependence of CISS in experiments¹²⁶, much of biomolecular-CIIS as observed is a non-equilibrium phenomenon where the effects of electron correlations and electron structure in materials cannot be neglected. Accounting for these likely-more-significant contributions calls for a different approach.

D. CISS in Waveguides: Coarse-Grained Models

While continuum models are useful in distilling geometric contributions to CISS and scattering effects, electrons do not simply tunnel through free-space nor along helical waveguides. For non-excited state transfer, transmission is mediated via both through-space and through-bond couplings, the latter of which arises from orbital interactions. From this, two general mechanisms of electron transport may feature: (a) a coherent, single-step tunnelling process, predominant at short distances/lengths; (b) an incoherent, thermally-activated multi-step hopping scheme; alongside intermediate mechanisms (structural fluctuation-induced ‘flickering resonance’ etc.). Though schema have been devised to determine which mechanisms dominate in an experimental set-up¹²⁷, it would be desirable to arrive at numerical transport predictions. Here, a coarse-grained approach employing tight-binding models captures core elements of actual setups while keeping flexibility and tractability in adjusting parameters. Prototypical efforts in this vein were given by Gutierrez *et al.*¹²⁸ and Guo & Sun¹²⁹; both of which made use of simplified single-orbital/channel tight-binding models, featuring

Description	Expression
Kane-Mele-like	$\sum_m i\lambda \psi_m^\dagger (\vec{\delta}_1 \times \vec{\delta}_2) \cdot \vec{\sigma} \psi_{m+2} + \text{H.c.}$
Rashba-like	$\sum_m i\lambda \psi_m^\dagger (\sigma_m + \sigma_{m+1}) \psi_{m+1} + \text{H.c.}$
Aharonov-Casher	$t \sum_m \psi_m^\dagger \psi_{m+1} + \text{H.c.} \rightarrow t \sum_m \psi_m^\dagger e^{i\lambda (d_{m,m+1} \times \mathbf{E}_{m,m+1}) \cdot \vec{\sigma}} \psi_{m+1} + \text{H.c.}$

TABLE I. Phenomenological SOC expressions

parameterized coupling strengths and variable SOC schemes (Fig. 12). The leads can be accounted for explicitly, and transmission spectra and a projected local density-of-states of the entire apparatus can be treated by the Landauer-Buttiker formalism, or non-equilibrium Greens’ function methods to account for dissipative effects. Of particular note, the literature features a broad array of SOC quantization schemes, each reflecting the background under which CISS is being treated. A number of such bare-SOC descriptions are stated in Table I, each corresponding to a subtly different physical picture, making comparison between models somewhat tenuous: the Kane-Mele-like expression considers intrinsic SOC in which inversion-symmetry negates nearest-neighbor SOC coupling and leaves only next-nearest-neighbor (NNN) SOC terms surviving; the Rashba-like expression instead assumes the Frenet-Serret frame and computes a nearest-neighbor SOC component between the rotated spinors; and in a similar vein, the Aharonov-Casher-like phase description is motivated by the fact that an applied electric field $F(t)$ is proportional to the time derivative of the time-dependent vector potential $\mathcal{A}(t)$ via $F(t) = -c^{-1} \partial_t \mathcal{A}(t)$, such it augments the nearest-neighbor hopping term by a factor $\exp[i\gamma \mathcal{A}(t)]$ and explicitly breaks time-reversal symmetry.

It can be argued that choice of (bare-)SOC scheme does not affect the overall physics of a CISS model given the low orders of SOC coupling, though a symmetry analysis from Kohn-Sham DFT calculations by Zöllner *et al.*¹³⁰ suggests that imaginary components of an SOC field lead to nonsymmetric Green’s functions/propagators that give rise to finite spin-current. Regardless of the uncertainty on SOC and geometric contributions, it is generally agreed that bare-SOC cannot make up for the anomalous extent of spin-selectivity observed in the ambient noisy conditions CISS remains stable under. Much of the theoretical literature revolves around the search for the missing link to bridge CISS’s strength gap alongside other key features, with coarse-grained models covering a vibrant exchange of ideas owing to the convenience the method affords. Early efforts from Gutierrez *et al.*¹²⁸ to build a minimal model for CISS use a Peierls-substitution SOC scheme to suggest that despite low SOC strengths, small charge-mobility (due to weak dispersion) enhances the extent of spin-flip/rotation in a general model, benchmarking spin-polarization to average spin-transmission asymmetry. This is immediately challenged by Guo & Sun¹²⁹ who, featuring a second-quantized SOC scheme on a rotating frame, surmise that, for dissipationless single-channel models with ideal unpolarized leads, the SOC field can be removed by a unitary transformation that recasts the system in a rotating frame following spin precession (additionally, CISS was benchmarked

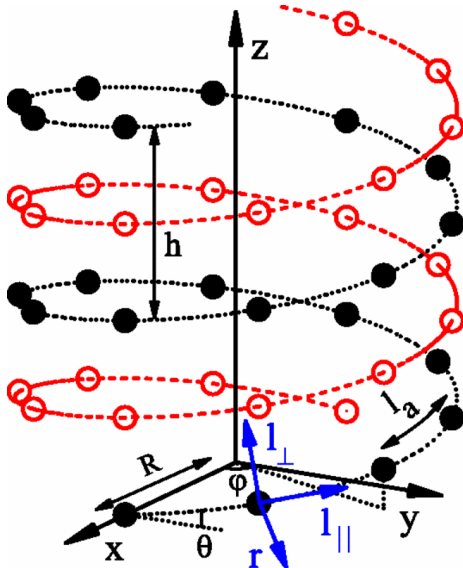


FIG. 12. Guo & Sun’s (2012a) tight-binding model of CISS, where each atom is modeled by a node fitted with its own Frenet-Serret frame, parametrized by a path variable (φ). Each Frenet-Serret frame is oriented such that the tangent unit-vector is tangential to the helix. Reprinted with permission from Guo & Sun¹²⁹, Physical Review Letters **108**, 218102 (2012). Copyright 2012 American Physical Society.

here using charge-conductance anisotropy). The contrast between these two works sets some basic conditions around which further coarse-grained models build:

- for single-channel models, dephasing¹³¹ or decoherence (arising from electron-phonon or electron-electron interactions, etc.) is necessary to break Kramers’ degeneracy produce spin-selectivity;
- time-reversal symmetry on the Hamiltonian level is assumed to hold under a lack of external field application;
- while the leads may be considered unpolarized to isolate helical contributions to spin-selectivity, this is only justified if non-linear response sources (i.e. bridge polarizability, charging effects, electron-electron correlation) and non-equilibrium effects such as electron-reorganization or bridge-deformation can be neglected, which may no longer correspond to realistic pictures;
- either spin-resolved transmission or spin-current anisotropy or charge-current anisotropy is used to benchmark spin-selectivity in CISS models, none of which are equivalent to each other.

In effect, a coarse-grained approach lends well to studying idealized scenarios or a ‘part-by-part’ investigation of CISS. Using parameterized coupling strengths derived from experimental results and ab initio calculations, Guo & Sun explored physically-motivated double-stranded (dsDNA: 2012a,b)^{129,132} and single-stranded models (polyalanine: 2014)⁸⁵. However, given bare-SOC’s inability to account for CISS’s anomalous spin-selectivity, future analytic phe-

nomenological models have since shifted to investigating model additions or specific interaction contributions. To summarize explorations within this line:

- multi-terminal effects on single-channel models have been found to cause dephasing via interference like Buttiker virtual leads^{85,133};
- modeling transport across multiple orbitals (often the three p-orbitals) allows for finite spin-selectivity with fully-coherent transport⁷³ since SOC can no longer be removed by a gauge transformation. This has also been demonstrated using explicit Slater-Koster formulation of orbital-overlaps, accounting for the exact paths by which SOC emerges and deriving effective couplings^{134,135}; alternatively, a large effective SOC may arise from spontaneous formation of electron-hole pairs between s- and p-orbitals¹³⁶.
- electron-lattice interactions can greatly enhance spin-selectivity owing to lower charge-mobility. Electron-phonon interactions in particular can induce indirect electron-electron attraction, leading to exchange splitting across spin channels that culminates in a temperature-activated/vibrationally-assisted spin-selectivity^{20,21,137–139}. Such electron-lattice coupling can also be represented by non-adiabatic coupling to nuclei that manifest as a finite Berry curvature^{108,109,140}, or phenomenologically described by a dissipative frictional non-linear potential¹⁴¹.
- polaron formation (where applicable from strong coupling between electron and lattice) is proposed to induce spin-momentum locking in which an “inverse Faraday effect” favors spin-flips and suppresses backscattering due to the relatively large mass of polarons, indirectly enhancing spin coherence¹⁴²;
- similarly, electron-electron correlations (Coulomb interactions) can also enhance spin-selectivity by inducing spin-asymmetric spectral weights while also being sensitive to external magnetic conditions such as lead polarization^{143–145};
- non-equilibrium conditions (i.e. presence of a bias field) are necessary for CISS as detailed by Wolf *et al.*⁷⁴, unless an external magnetic flux is applied¹⁴⁶. Additionally, Fransson^{15,137,143} argues strongly and are the first to account for the presence of ferromagnetic or polarized-leads. Dalum & Hedegard⁹⁰ go further to explicitly demonstrate that CISS alters magnetization/polarization in the leads due to electron-reorganization.
- many miscellaneous studies including: contact/lead chirality effects¹⁴⁷; gate voltage effects¹⁴⁸; spin-current-induced mechanical torque¹⁴⁹; spin-current-induced charge-current^{94,150}; chiral phonon effects^{69,151} (see Wang *et al.*, 2024¹⁵² for a broad overview); waveguide-transfer effects¹⁵³; Floquet-driving effects^{154,155}; realization of Majorana

modes¹⁵⁶; an explicit Lindbladian treatment with dephasing¹⁵⁷; et cetera.

Aside from a handful of works that treat CISS as a fundamental mirror-symmetry breaking phenomenon in search for a general theory closer to application in chiral crystals or inorganic chiral nanowires, many efforts strive to account for CISS as observed in biomolecular experiments. In this regard, tight-binding models are ill-at-ease with deformable biomolecules and similar dielectric soft matter. *ab initio* numerical techniques present a powerful avenue in accounting for these details and have already been employed to study symmetry or conformational effects^{84,130}, interface effects¹⁵⁸, and the role of many-body exchange interactions¹⁴⁴ in CISS, with Dednam *et al.*¹⁴⁷ showing that achiral molecules can give rise to spin-polarization if the leads/contacts are chiral.

Additionally, there has also been a vigorous thrust to reconsider CISS's identity as a spin-selectivity phenomenon and broaden it to include orbital-selectivity due to spin-orbital mixing by SOC. This line of argument stems back to the earliest theoretical work on CISS by Skourtis *et al.*¹⁵⁹, in which they propose that enhancement of CISS-transmission via circularly-polarized light of the matching helicity operates via ‘current transfer’: or the (partial) conservation of angular-momentum as electrons transfer from a donor to a bridge. Following up on this, Gersten *et al.*¹⁰¹ analytically study how spin-selectivity in CISS arises from interfacial spin-orbit coupling and orbital angular-momentum selection by the molecular bridge’s helical geometry, showing that they eliminate the need for dephasing or inelastic effects. This culminates into Liu *et al.*’s⁷⁰ argument that in CISS, the chiral molecule acts primarily to select orbital angular momentum, inducing a topological orbital texture that is reliant on inversion-symmetry breaking rather than strict helical geometry; spin-selectivity is conferred by SOC in the leads or at the interface, forgoing reliance on the low SOC strength of chiral biomolecules altogether. Experimental encouragement for this viewpoint has been found in the efforts of Adhikari *et al.*¹⁰⁵, where use of a low-SOC substrate (Al) did not generate CISS in MR-response as compared to Au. While the microscopic picture of how a chiral, not necessarily helical, geometry influences spin-dynamics remains unclear, there are strong signs that the orbital degree-of-freedom cannot be neglected and that CISS should be viewed as a generalized angular-momentum phenomenon. This detour highlights the importance of whole-setup effects, which we explore in more detail in the next section.

E. CISS-on-Substrates: Pictures-in-Motion and Extra-Molecular Effects

While coarse-grained models are instructive in determining the necessary conditions to and contributors for CISS, most of them fall short in accounting for its non-equilibrium, non-linear behavior, compounded by whole set-up effects that cannot be ignored in trying to account for CISS’s strength. In the absence of powerful ab-initio methods that can simu-

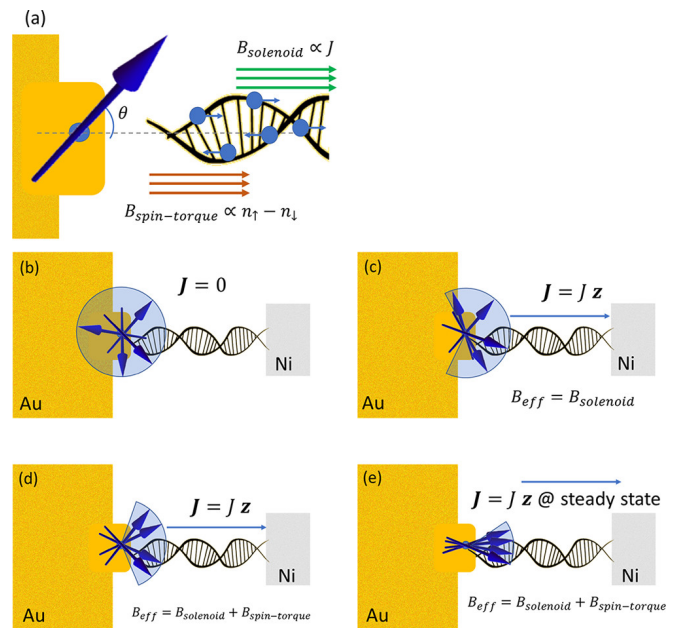


FIG. 13. Alwan & Dubi’s (2021) dynamical on-bias interfacial model, depicting how a magnetic moment arises at substrate surface-states, bolstering spin-selectivity in CISS-junction setups. When bias is applied and charge-current is finite across the junction, a magnetic order is generated within the CISS molecule such that it exerts a solenoid-like magnetic field on the substrate surface. Given the magnetic polarizability of the substrate, this tilts magnetic dipoles of the surface states towards the molecular axis. This in turn further magnetizes the chiral bridge, and the resulting feedback mechanism is analogous to spin-transfer torque. Reprinted with permission from Alwan & Dubi⁶¹, Journal of the American Chemical Society 143, 14235-14241 (2021). Copyright 2021 American Chemical Society.

late entire CISS set-ups, what is necessary to better understand non-equilibrium effects in CISS and distill their contributions are time-dependent models. Several coarse-grained models already attempt to account for CISS across both the transient and steady-state regimes¹⁵, but they stop short of bridging the ‘strength gap’ in CISS. Here, Alwan & Dubi⁶¹ propose that CISS’s anomalous spin-selectivity as experimentally observed arises from a spin-torque feedback mechanism between the substrate and the molecular bridge, using self-consistent mean-field calculations to calculate steady-state magnetocurrent anisotropy (Fig. 13). When an initial spin-current passes through the helical bridge, it sets up a small magnetic moment in the bridge, acting as an effective solenoid field that interacts with the initially randomly-aligned substrate surface orbitals. This aligns the orbitals, setting up an effective interfacial magnetic moment that increases the spin current, thus amplifying the effective interfacial magnetic field to strengths that can account for experimental levels of spin-selectivity in molecular junctions.

Within its purview, the spin-torque feedback mechanism can be employed to rationalize several experimental observations of CISS-transport^{62,68,160}. It of course does not provide any concrete explanation as to the origin of the effect, since

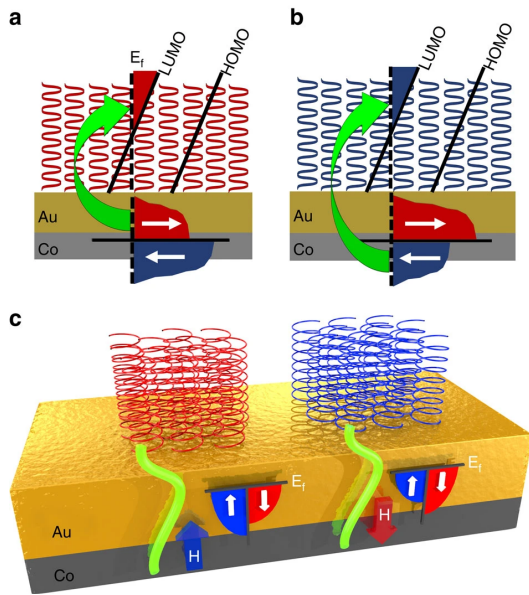


FIG. 14. Ben Dor *et al.* (2017) on-attach interfacial MIPAC model, describing how a magnetic order may be established on a substrate upon adsorption of a chiral film. Beginning from the premise that the chiral monolayer possesses a nontrivial dipole moment, charge transfer occurs to equalize the electrochemical potential of the adsorbed layer and the substrate surface, and this is spin-selective due to CISS in their account. One may relax this premise by instead accounting for interfacial wavefunction spread as offered by Zhao *et al.* (2025). Reprinted with permission from Ben Dor *et al.*³³, Nature Communications **8**, 14567 (2017). Copyright 2017 Authors, licensed under a Creative Commons Attribution (CC BY) license.

CISS has been observed in substrates with negligible SOC¹⁰⁵. Observations of anomalous spin-selectivity upon incidence of linearly-polarized light in CISS-photoemission eludes a junction-based description, suggesting the chiral layer induces a persistent magnetic order in its substrates even at zero-bias. The latter was corroborated by observations of finite CISS-dependent Hall-response in a metal-substrate-SAM device without bias nor external magnetic field application³³, alongside direct observations of magnetization re-ordering and flipping upon adsorption of chiral molecules^{161,162}. Remarkably, MIPAC experiments by Meirzada *et al.*³⁴ then demonstrated that the induced magnetic-order is transient but can be long-lived, persisting over a period of days (the strength of which is correlated with the contact angle between chiral molecule and substrate). While analytic treatments of CISS's stable non-equilibrium effects remain to be developed, heuristics offer possible explanations. For instance, Ben Dor *et al.*³³ propose that it owes to a spin-dependent proximity effect: the electron wavefunctions of the underlying ferromagnet delocalize into the SAM through the Au substrate (Fig. 14). The extent of penetration is spin-dependent due to the chiral layer, inducing an imbalance of spin-populations in the ferromagnet, thus setting a magnetic order; which is analogous to the charge-trapping model by Zhao *et al.* previously detailed in Sec. II B. They make an equivalent semiclassical argument: the SAM dipoles lower the LUMO below the device's Fermi level, in-

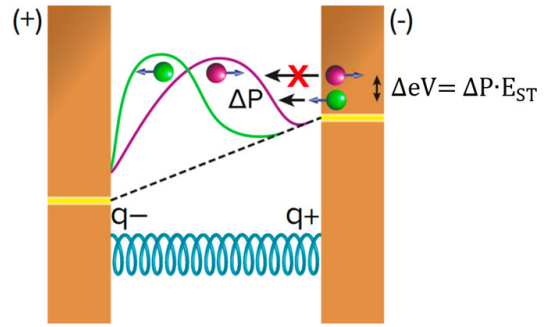


FIG. 15. Illustration of Naaman *et al.*'s (2020) spin blockade model. Spinor wavefunctions penetrate differentially through a dielectric chiral bridge, with the unfavored spin being localized closer to the donor, resulting in a spin-blockade forming for the unfavored spin (due to Pauli's exclusion principle). Reprinted with permission from Naaman *et al.*⁵⁷, The Journal of Physical Chemistry Letters **11**, 3660-3666 (2020). Copyright 2020 American Chemical Society, licensed under a Creative Commons Attribution (CC BY) license.

ducing electrons to transfer from the FM, with stimulated spin-splitting due to CISS occurring in the process. Meirzada *et al.*³⁴ elaborate on this, suggesting that large spin-exchange energies stabilize the transient magnetization¹⁴⁴, with the order eventually decaying via intrinsic Gilbert damping and thermalization of spin states^{163,164}.

At this juncture, it is evident that charge-redistribution plays a crucial role in CISS-transport, one that is difficult to capture by general equilibrium models. Proposing an explanation for this, Naaman *et al.*⁵⁷ offer the local spin-blockade picture, illustrated in Fig. 15. The picture occurs in two stages: in-bridge spin-dependent charge-reorganization (SDCR) and into-bridge injection. Firstly, upon application of the bias field across a CISS-junction device, an electric dipole is set up within the chiral molecule, and charge-redistribution occurs. Due to CISS, the charge-redistribution is spin-dependent, such that electrons of the preferred spin delocalize further along the molecule than the non-preferred spin. Thus, the bridge sites closest to the donor electrode are preferentially populated by the non-preferred spin upon reorganization, giving rise to an interfacial “spin blockade”. In the next stage, an electron from the donor is injected into molecule, experiencing a spin-dependent tunneling barrier, the energy difference of which can be expressed as $SP(V) \cdot \Delta E_{S,T}$. In words, the injection step is likened to the formation of either a singlet pair or a triplet pair, by sheer proximity, with the unpreferred ‘local’ spin at the interface. Preferred ‘excess’ spins from the donor form a singlet, while the unpreferred counterpart forms a triplet, with the energy difference being $\Delta E_{S,T}$. Thus, injected electrons not only encounter the initial spin-dependent barrier owing to the chiral bridge’s intrinsic SOC, it also faces an additional ‘spin blockade’ due to the singlet-triplet formation at the interface, drastically increasing spin-selectivity. Since the charge-reorganization step does not necessarily give rise to a ‘perfect spin-blockade’, a bias-dependent initial spin-separation index, $SP(V)$, is used as a scale factor.

In alignment with Zhao *et al.*⁸⁷, the spin-blockade picture

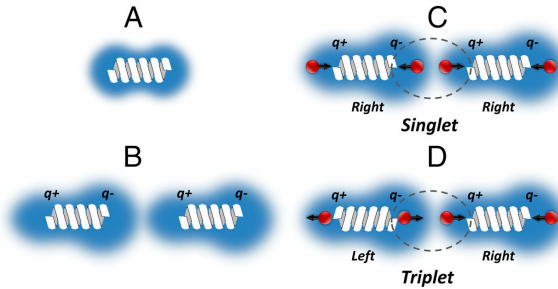


FIG. 16. Illustration of Kumar *et al.*'s capacitative spin-dependent charge-reorganization. Due to dispersion forces, induced dipoles are generated in two proximal chiral molecules, generating singlet or triplet states depending on the helical-sense matching. Reprinted with permission from Kumar *et al.*³², Proceedings of the National Academy of Sciences **114**, 2474-2478 (2017). Copyright 2017 National Academy of Sciences, licensed under a Creative Commons Attribution (CC BY) license.

accounts for observations of nonlinear response via the bias-dependent tunneling barrier, while magnetocurrent anisotropy readings are also predicted to fall at high bias voltages since the spin-blockade is no longer energetically comparable. It remains unresolved how the differences between the spin-blockade picture and the charge-trapping picture mean translate to their use in physical modeling. A finer outlook would require explicitly accounting for exchange interactions¹⁵, highly-dielectric behavior, and possible long-range hopping or through-space contributions to transport.

F. CISS beyond Substrates: Chiral Transmission and Proximal Dispersion Forces

One topic has remained conspicuously missing from our coverage thus far: how does CISS feature in biological processes? This topic has long been a central pillar in CISS focuses due to the as-yet unrealized potential of spin-manipulation in biochemical processes; but due in part to difficulty of experimental realization of CISS in biology^{165,166}, insight into its effect on bare molecules is often derived indirectly. As such, much of our preceding discussion has centered around chiral molecules adsorbed on substrates. For all its promise, work on CISS-beyond-substrates is still nascent; but it has nevertheless already given plentiful insight on CISS, one part of which is its role in enantioselection¹⁶⁷.

For one, it is well-known that chiral macromolecular structures can spontaneously self-assemble from chiral monomers or achiral monomers in chiral media (see Liu *et al.*⁴ for reference). Does CISS mediate this? Or specifically, can CISS occur between capacitatively-coupled molecules? Introduced by Michaeli *et al.*¹⁶⁸ and Kumar *et al.*³², capacitative SDCR was proposed to occur when two chiral molecules are brought into proximity with significant overlap of electronic wavefunctions (Fig. 16). In brief, the molecules interact via attractive dispersion forces, setting up an induced-dipole in each molecule and inciting charge-redistribution within each

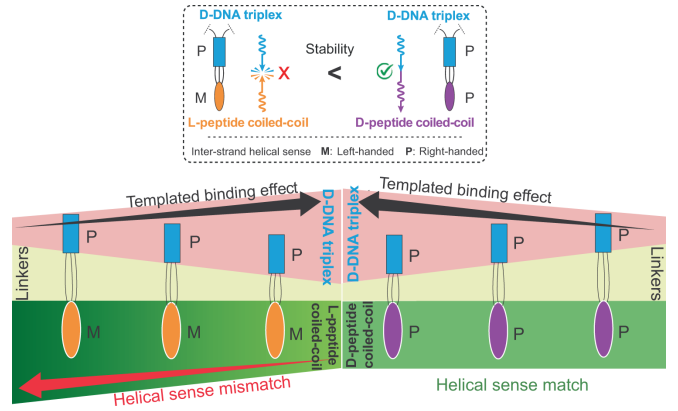


FIG. 17. Graphical summary from Pandey *et al.* on chiral-to-chiral communication propagating between two bio-macromolecular domains (DNA triple helices and peptides). The strength of the cross-strand linkage weakens with increasing linker length more drastically when the domains have different screw-sense helicity, suggesting a long-range electronic mechanism at play. Reprinted with permission from Pandey *et al.*⁴¹, Nature Communications **13**, 76 (2022). Copyright 2022 Authors, licensed under a Creative Commons Attribution (CC BY) license.

molecule. Due to CISS, the charge current is accompanied by spin-separation, forming singlet/triplet regions between the molecules if they are of the same/different chiral sense. This constitutes an enantioselective interaction that preferentially stabilize biomolecular-bonding due to different spin-correlation energies. However, calculations from Geyer *et al.*¹⁶⁹, peg the magnetic response from these fluctuations to be weaker than London forces, and Hedegard¹⁷⁰ elaborates how the effect is too weak to influence chemical reactions for SOC strength and dipole-matrix elements to order $\sim 10^{-3}$ eV, and excitation energies to order ~ 1 eV.

While spin fluctuation-induced proximity effects may be negligible in chiral transmission, this does not preclude the presence of long-range interactions. For this, we may consider an alternative scenario: does CISS mediate bond-breaking of two covalently-bound chiral/helical molecules?

Remarkably, Pandey *et al.*⁴¹ demonstrated that helical-sense matching affects bonding strength even when the helical biomolecules are bonded through a linker and separated beyond the effective range of dispersion forces (Fig. 17). The mechanism behind this behavior is unclear, but we may indirectly take our cue from analyses focusing on with-substrate force spectroscopy: Kapon *et al.*¹⁴⁵, studying atomic force-microscopy (AFM) CISS experiments, proposes that dispersion forces are supplemented by spin-exchange interactions, generated by the onset of polarized singlet states, giving rise to long-range magnetic interactions that correspond to chiral-discrimination in AFM settings. This result is further buttressed by Safari *et al.*¹⁷¹, in which significant magnetoconductance anisotropy was found for single-molecule AFM setups at low temperatures of 5K, precluding contribution from electron-phonon interactions and ensemble effects that appear as confounders for setups utilizing chiral nanolayers.

In light of these two perspectives, one may recognize proximal dispersion forces and exchange interactions are significant in chemisorption and enantioselectivity, but observations of these at work are facilitated by some form of contact, direct or indirect. Is this indicative of biomolecular CISS processes likely requiring indirect contact, or is there a possibility for appreciable non-local CISS effects in biology? And in either case, how can we better account for chiral transmission via self-assembly and broader biomolecular processes?

G. CISS in Spin Chemistry and Electron Transfer Reactions

CISS has been proposed to be of relevance to several electron transfer reactions in biological systems, such as DNA, photosystem I, and cryptochrome, as well as artificial systems, such as quantum dots. While the underlying theory of electron transfer is well established^{172,173}, its interplay with CISS is still a developing field. In this section we explore some of the emerging models. Chiesa *et al.*¹⁷⁴ defined a set of output states in proposed experiments to interrogate potential CISS effects in electron transfer processes through a chiral bridge linking a donor and acceptor pair. In particular, they identify a polarized state as arising from a spin filtering process through a chiral bridge with associated density matrix

$$\rho_0^{(F)} = \begin{pmatrix} 0 & 0 & 0 & 0 \\ 0 & \frac{1+p}{2} & 0 & 0 \\ 0 & 0 & \frac{1-p}{2} & 0 \\ 0 & 0 & 0 & 0 \end{pmatrix},$$

taken in the standard basis two-spin basis of $\{| \uparrow\uparrow \rangle, | \downarrow\uparrow \rangle, | \uparrow\downarrow \rangle, | \downarrow\downarrow \rangle\}$ and satisfying $-1 \leq p \leq 1$ and $p \neq 0$. The final polarization of the acceptor here is given by $p = -2\text{Tr}[\rho_0^{(F)} S_{zA}]$. By designing magnetic resonance experiments^{175,176}, they aimed to distinguish outputs in terms of this polarized state, a singlet state, and a non-Boltzmann but unpolarized state, to determine whether the electron spin is polarized after electron transfer^{177,178} through a chiral bridge.

In addition to spin filtering mechanisms, spin coherent mechanisms have also been proposed. Luo & Hore¹⁷⁹ formulated a phenomenological model, to investigate CISS effects in cryptochrome magnetoreception, that assumes spin polarization during the formation and recombination of a singlet born radical pair. Formally they arrive at the initial state

$$|\psi_0\rangle = \cos\left(\frac{\chi}{2}\right) |S\rangle + \sin\left(\frac{\chi}{2}\right) |T_0\rangle, \quad (22)$$

where $|S\rangle$ denotes the spin singlet state, $|T_0\rangle$ the spin triplet state, χ parametrizes the extent of spin-selectivity, and a recombination projection operator $P_R^{(P)} = |\psi_R\rangle\langle\psi_R|$, where

$$|\psi_R\rangle = \cos\left(\frac{\chi}{2}\right) |S\rangle - \sin\left(\frac{\chi}{2}\right) |T_0\rangle. \quad (23)$$

In comparison to the model introduced by Chiesa *et al.* the

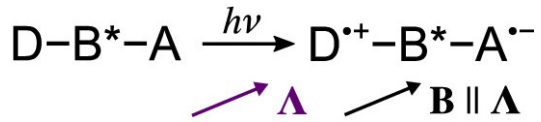


FIG. 18. Simple schematic of the radical-pair mechanism: when a donor and acceptor molecule, covalently linked by some chiral bridge, is photoexcited to generate a radical pair, the system then forms a charge transfer state. Direct diabatic coupling provides singlet character, while SOC (Δ) contributed by the chiral bridge provides triplet character, with chirality altering the phase sign. No spin-polarization emerges, but instead spin-coherence. Application of a magnetic field parallel to the SOC breaks time-reversal symmetry of the Hamiltonian and allows for decay of coherence, which can then be experimentally probed by electron paramagnetic resonance setups. Adapted with permission from Fay¹⁸⁴, The Journal of Physical Chemistry Letters **12**, 1407-1412 (2021). Copyright 2021 American Chemical Society.

corresponding density matrix is given by

$$\rho_0^{(P)} = \begin{pmatrix} 0 & 0 & 0 & 0 \\ 0 & \frac{1+\sin\chi}{2} & -\frac{\cos\chi}{2} & 0 \\ 0 & -\frac{\cos\chi}{2} & \frac{1-\sin\chi}{2} & 0 \\ 0 & 0 & 0 & 0 \end{pmatrix}.$$

Using this formalism, Luo & Hore demonstrated that external magnetic field sensitivity can be enhanced in radical pairs subject to strongly asymmetric recombination. Further studies by Tiwari, Raghuvanshi & Poonia^{180,181} extended upon this result and suggested that CISS may amplify the relative entropy of coherence for both the electronic subsystem alone and the combined electronic-and-nuclear system, and have applied the model to planaria regeneration¹⁸². Nonetheless, open questions remain for the role of CISS in electron transfer reactions in biophysical processes. These include identifying the correct theoretical framework and establishing if predictions are consistent with previous observations, and experimental verification of CISS effects, for which interpretations of EPR spectra of photosynthetic bacterial reaction centers revealed no significant CISS generated polarization¹⁸³.

Another spin coherent mechanism was introduced by Fay¹⁸⁴ who demonstrated that, based on a microscopic derivation for a one-step electron transfer in radical pairs, chirality in conjunction with SOC generates quantum coherence between singlet and triplet spin-states, yet does not generate spin polarization; we briefly detail the model as illustrated in Fig. 18.

Consider a charge-transfer reaction for a photoexcited radical pair system. The excited precursor state can be designated $|0\rangle = |DA^*\rangle$, and the charge-separated radical-pair state can be designated $|1\rangle = |D^{\bullet+}A^{\bullet-}\rangle$, where $D(A)$ indicates the donor(acceptor). Of note, $|0\rangle$ only exists in the singlet configuration while $|1\rangle$ can exist in either singlet and triplet configuration. The Hamiltonian for such a system dressed in an SOC field is thus:

$$H = H_0\Pi_0 + H_1\Pi_1 + V, \quad (24)$$

where $H_m \Pi_m$ denote the Hamiltonian and projection operators onto charge-transfer state m , with $H_m = H_{ms} + H_{mn}$ accounting for both electron and nuclear spin subspaces while $\Pi_0 = |0\rangle\langle 0|\hat{P}_S$ and $\Pi_1 = |1\rangle\langle 1|(\hat{P}_S + \hat{P}_T)$ account for each state's allowed spin-multiplicity through the singlet(triplet) projection operators $\hat{P}_S(\hat{P}_T)$. V consists of our potentials of interest, the spin-conserving diabatic coupling V_{DC} and SOC:

$$\begin{aligned} V &= V_{DC} + V_{SOC} \\ &= \Delta (\hat{P}_S |0\rangle\langle 1| + |1\rangle\langle 0|\hat{P}_S) - i (\hat{P}_S |0\rangle\langle 1| \boldsymbol{\Lambda} \cdot \hat{\mathbf{S}}_1 - \boldsymbol{\Lambda} \cdot \hat{\mathbf{S}}_1 |1\rangle\langle 0|\hat{P}_S) \\ &= \Gamma (\hat{P}_S |0\rangle\langle 1| \hat{U}^\dagger + \hat{U} |1\rangle\langle 0|\hat{P}_S), \end{aligned} \quad (25)$$

with $\boldsymbol{\Lambda}$ being a real-valued momentum-dependent vector coupling and $\hat{\mathbf{S}}_1$ being the spin-operator on a particular electron denoted '1' in the electron-transfer process, giving $\hat{U} = (\Delta + i\boldsymbol{\Lambda} \cdot \hat{\mathbf{S}}_1)/\Gamma$ and $\Gamma = \sqrt{\Delta^2 + |\boldsymbol{\Lambda}|^2/4}$.

Physically, \hat{U} acts to rotate electron spin about an axis $\hat{\mathbf{n}} = \boldsymbol{\Lambda}/|\boldsymbol{\Lambda}|$ for an angle $2\theta = 2 \cdot \arctan(|\boldsymbol{\Lambda}|/2\Delta)$. Additionally, opposite enantiomers, denoted by + and -, have opposite $\text{sgn}(\boldsymbol{\Lambda})$ such that $\boldsymbol{\Lambda}_+ = -\boldsymbol{\Lambda}_-$. Proceeding to solve the Nakajima-Zwanzig equations for the system, under the Markovian assumption and that the reaction is instantaneous and irreversible (i.e. $k_b \rightarrow 0$), Fay obtains:

$$|\psi_0^\pm\rangle = \cos \theta_+ |S\rangle \pm i \sin \theta_+ |T_0(\mathbf{n}_+)\rangle, \quad (26)$$

$|T_0(\mathbf{n}_+)\rangle$ the triplet-state defined along the axis \mathbf{n}_+ , and $|\psi_0\rangle = \hat{U} |S\rangle$ the initial spin state of the system. In comparison to the previous initial states Fays model gives the initial density matrix

$$\rho_0^{(C)} = \begin{pmatrix} 0 & 0 & 0 & 0 \\ 0 & \frac{1}{2} & -\frac{1}{2}(\cos \chi + i \sin \chi) & 0 \\ 0 & -\frac{1}{2}(\cos \chi - i \sin \chi) & \frac{1}{2} & 0 \\ 0 & 0 & 0 & 0 \end{pmatrix}.$$

Effectively, in the absence of any incoherent (i.e. dissipative) process, Fay's radical pair model demonstrates that CISS is only spin-selective for coherence and not for polarization, a conclusion in line with analysis in Sec. II A. Fay & Limmer¹⁸⁵ then extended upon this result by considering a two-step model to describe CISS-photoemission (Fig. 19), likening the process to chemically-induced dynamic electron-polarization¹⁸⁶. In brief, by introducing an additional exchange coupling term between donor and acceptor spins in the radical pairs, the triplet state now has an oscillating real part; this oscillating spin polarization is subsequently converted into a static quantity via a final incoherent electron-transfer step. Furthermore, the model was shown to have a temperature dependence consistent with experimental results by Carmeli *et al.* on CISS in electron transfer in photosystem I⁶⁷. In a subsequent work, Fay & Limmer explored the role of CISS in charge recombination, and a reaction operator was derived that described superechange and incoherent hopping limits¹⁸⁷. Most recently, this framework has also been extended to demonstrate enantioselectivity via CISS and thereby

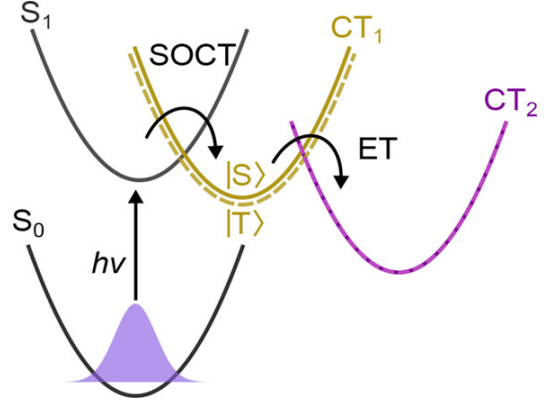


FIG. 19. Schematic for conversion of chiral-induced spin-coherence to CISS via a final incoherent step. In realistic conditions, the radical-pair undergoes multiple downhill electron transfers, resulting in a final well-separated ion pair. This can be modeled by adding a final dissipative or incoherent electron transport step that generates spin-selection from spin-coherence. Reprinted with permission from Fay & Limmer¹⁸⁵, Nano Letters **21**, 6696-6702 (2021). Copyright 2021 American Chemistry Society.

give rise to new methods for asymmetric synthesis using spin-polarized electrons¹⁶⁷.

Although, the CISS models that generate polarization or only coherence give rise to distinct initial states, by combining a local phase rotation operation on a transferred electron in combination with evolution under exchange coupling, Smith *et al.*¹⁸⁸ have provided a unified scheme that allows interpolation between these models. Using this, they have also extended to accommodate triplet precursor radical pairs, allowing effects due to spin selectivity in polarization or coherence to be identified and the underlying conditions for enhancements in magnetic field sensitivity and coherence to be elucidated in radical pairs in cryptochrome. Recently, Eckvahl *et al.*³⁹ produced evidence of a direct observation of CISS in intramolecular electron transfer for an isolated, photoexcited chiral molecule within a liquid crystal medium. Specifically, they used time-resolved electron paramagnetic resonance (TREPR) spectroscopy to identify signatures of the CISS effect on the spin states of spin-correlated radical pairs by rotating the molecules relative to an applied magnetic field (Fig. 20). While the model of Luo & Hore is used for comparison, the authors state that the models discussed in this section, i.e. associated with $\rho_0^{(F)}$, $\rho_0^{(P)}$, and $\rho_0^{(C)}$, are equivalent for describing the TREPR spectra provided that polarization effects are incorporated. However, by comparing these density matrices, we see that the models are not equivalent and differ with respect to coherence elements. Although not relevant for the interpretation of TREPR, these differences could potentially be of importance for applications utilizing quantum resources, such as quantum sensing or quantum information protocols like quantum teleportation^{66,189}. In Sec. IV B, we revisit model differences in CISS to discuss a scenario in magnetic field sensing where stark differences can arise if CISS is selective for polarization or coherence only.

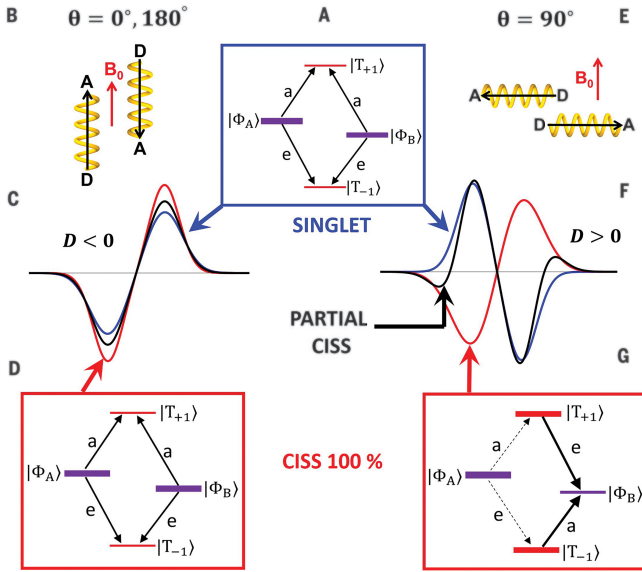


FIG. 20. The effect of CISS on the spin states of spin-correlated radical pairs (SCRPs), as revealed by time-resolved electron paramagnetic resonance (TREPR). (A) In the absence of CISS, a SCRP formed in a singlet state evolves in the presence of a strong static magnetic field \mathbf{B}_0 . (B, E) Alignment of the chiral molecules parallel ($\theta = 0^\circ, 180^\circ$) or perpendicular ($\theta = 90^\circ$) to \mathbf{B}_0 . (C, F) TREPR spectra showing singlet-born SCRP signals with and without CISS contributions, where red traces indicate full CISS generated spin polarization, black traces indicate partial CISS contributions, and blue the case without CISS. (D, G) Schematic diagrams of spin states under 100% CISS contribution. D represents spin-spin interactions. Reprinted with permission from Eckvahl *et al.*, Science **382**, 197–201 (2023).³⁹ Copyright 2023 Authors.

Beyond the donor-bridge-acceptor context, quantum effects or enhancements have also been discussed in the context of CISS-transport through junctions. Wang *et al.*¹⁹⁰ identify that spin-polarization in CISS-transport can be induced and amplified by the presence of Fano resonances, arising from self-interference induced by a non-equilibrium distribution of injected states (i.e. optically excited) and further compounded by contributions from quasi-degenerate energy levels common in complex molecules¹⁹¹. In a similar vein, collected efforts from the Subotnik group^{108,109,140,192} raise the striking argument that failure of the nuclear-electronic adiabatic assumption can be a major contributor to CISS. In the vicinity of conical intersections, quasi-degenerate states can experience a significant Berry force, physically interpretable as a nuclear screening force acting on the electron¹⁹³, that can severely affect pathway selection of quantum states and potentially give anomalous spin-selectivity for small SOC strengths. Taken together, the results of this section highlight the substantial effects CISS may have on electron transfer reactions, and its observation at the molecular level demonstrates its potential in quantum technologies.

IV. BRIDGING THE GAP TO EMERGING APPLICATIONS: BIOMIMETICS, QUANTUM INFORMATION AND SENSING

Given the widespread manifestations of the CISS effect and its potential for spin manipulation, it is increasingly recognized not only for its fundamental significance but also for its potential in emerging quantum and molecular technologies, especially considering its reputed robustness at ambient temperatures. Applications span spintronics, including spin filters, spin valves, and spin-selective tunneling junctions, as well as chiral-induced spin light-emitting diodes (spin-LEDs), molecular switches, and enantioselective catalysts. Beyond device applications, CISS has also attracted attention in the context of biological electron transfer and the prospect of coherent control of chemical reactions. In this section, we maintain a focused discussion on sensing applications, quantum information and control concepts, and insights from biology¹⁹⁴, culminating in emerging spin-correlated radical pair platforms. Broader appraisals of CISS-enabled applications and implications are available in recent literature^{63,195–198}.

A. CISS-Inspired Sensing and Detection

Several proposed applications have emerged that harness the CISS effect's ability to polarize electron spins, enabling novel sensing and detection schemes. One promising route involves the utilization of magnetoresistive readouts and magnetoresistance properties of chiral systems^{93,199–203} for spintronic sensor development²⁰⁴. A particularly active area involves bioelectronic platforms²⁰⁵, where chiral molecules such as DNA hairpins²⁰⁶, peptides, or oligopeptides, serve as recognition elements along with spin-sensitive detection. These platforms present promising opportunities for biomedical diagnostics, offering spintronic alternatives to traditional label-based methods. In these efforts, Wang and co-workers proposed the use of a self-assembled monolayer of polypeptides and a CISS constructed Kerr technique to modulate incident linear polarized light on a non-magnetic metal surface with chiral molecules, where the deflection angle depends on the chirality of the molecule²⁰⁷.

DNA-based schemes are also undergoing rapid development, including investigations into CISS effects in Quantum Dot-DNA systems^{208,209} (Fig. 21), and CISS-based DNA hybridization sensors^{208,210,211}, which can be used to measure genetic similarity and finds several applications including drug discovery, pathogen detection, and hereditary disease diagnosis. Related strategies have demonstrated the detection of UVC-induced DNA damage via spin polarized electron signals²¹², potentially offering greater robustness over conventional electrochemical biosensors. Closely related is the concept of CISS-enabled enantioselective detection, where spin-polarized electron transport is influenced by the chirality of a target molecule, enabling enantiomer differentiation. Recent studies have explored spin-dependent enantiomeric separation^{42,43} and the use of nuclear magnetic resonance (NMR) as a tool for chiral sensing²¹³, with implications for

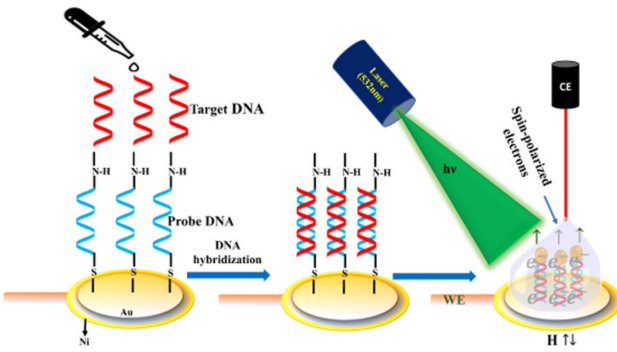


FIG. 21. Schematic of a CISS-based DNA hybridization sensor employing a quantum dot–DNA device. A probe single-stranded DNA (ssDNA) is immobilized on a gold-coated Ni substrate, followed by hybridization with target DNA. Upon illumination with circularly polarized light ($\lambda = 532$ nm), spin-polarized electrons are generated and transported through the hybridized double-stranded DNA (dsDNA). The CISS effect induces a differential change in charge-transfer resistance (ΔR_{ct}) between spin-up and spin-down electrons for both ssDNA and dsDNA, enabling spin-dependent detection of hybridization. This spin-selective readout enhances sensitivity over conventional charge-based methods and enables a detection limit as low as 10 fM under illumination. Adapted with permission from Bhartiya *et al.*²⁰⁸, Anal. Chem. **95**, 3656–3665 (2023). Copyright 2023 American Chemical Society.

chemical analysis and quantum information science.

Spin-selective photoluminescence presents another route for CISS-based sensing. Chiral organic emitters and perovskites can exhibit circularly polarized luminescence (CPL)^{214,215}, traditionally used to investigate chirality. However, CPL may also serve as a spin-based optical output in future sensor architectures (Fig. 22). Paralleling this, chiral hybrid perovskite systems have also seen use as spin light-emitting diodes^{48–52}, with Tang *et al.* reporting the first single-junction perovskite spin-LED operating at room temperature⁵², and with chiral SOC field strength later being shown to explicitly correlate with both external quantum efficiency and degree of circular polarization in electroluminescence, revealing a magneto-chiroptical interplay that can be tuned by compositional engineering⁵⁰. Overall, a number of studies have quantified the strength of chirality-induced spin-orbit coupling (CISOC) and its correlation to dimensionality, local inversion asymmetry, and electronic delocalization across chiral perovskites, thus paving the way for harnessing the CISS effect towards the development of practical spin-optoelectronic device architectures^{50,216}.

A theoretical basis for spin-polarized injection and circularly polarized electroluminescence in chiral perovskite spin-LEDs could be provided by modeling a spinor confined to a helical path, as considered recently by Ventra *et al.*²¹⁷, that naturally acquires a geometric chirality-induced spin-orbit coupling, expressed as $H_\chi = \alpha_\chi \hat{\sigma} \cdot \hat{p}$, with $\alpha_\chi \propto \kappa/R$ (over some curvature κ and radius R), enabling spin-momentum locking and breaking symmetry between T^\uparrow and T^\downarrow (which are the transmission probabilities for spin-

up and spin-down electrons, respectively) even in light-atom systems. This is further bolstered by findings from Zhang *et al.*¹⁵⁷ showing that asymmetric spin-velocities lead to a nonzero steady-state polarization $P_{\text{stat}} = (n_\uparrow - n_\downarrow)/(n_\uparrow + n_\downarrow)$, even without external magnetic fields. In fact, from a quan-

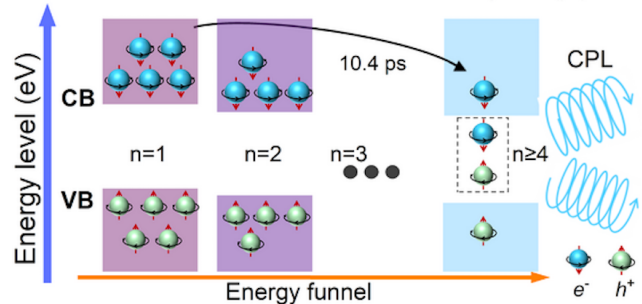


FIG. 22. A pictorial illustration for spin polarized exciton transfer and recombination in a high-performance sky-blue perovskite spin-LED due to chiral ionic liquid implantation and passivation. Adapted with permission from Zhang *et al.*⁵¹, Adv. Funct. Mater., 2503088 (2025). Copyright 2025 Wiley.

tum thermodynamic perspective, this implies that the state transformation mechanisms underlying the CISS effect could be acting as passive isothermal quantum erasers or initializers that are robust at room-temperature. In treating CISS as a quantum channel encoding spin-selective transmission amplitudes, chiral asymmetry due to molecular geometry, and open quantum systems effects like dephasing^{131,157}, one can conceptualise formally recasting it as an energetically optimal qubit transformer^{122,218}, thereby putting it in the same family as Landauer erasers, Maxwell's demon type quantum engines, and information-powered refrigerators.

Considered together, these developments demonstrate the versatility of the CISS effect for spin-selective sensing. Given the rapid growth and depth of the field, we have elected to highlight a few of these emerging sensing platforms, rather than an exhaustive coverage, which we hope provides some insight into the breadth of the field and potential applications, such as biomedicine^{219–221}. Further insight into quantum information and technology device implementation prospects of CISS can be found in several reviews^{26,189,195,196,222,223}. While many of these systems have not yet been investigated for active utilization of quantum resources, such as entanglement or coherence, their underlying quantum structure offers potential for quantum-enhanced sensing platforms²²⁰. In the following section we examine an emerging platform based on spin-correlated radical pairs, and explore the relation between quantum resources and sensing applications.

B. Spin-Correlated Radical Pair Platforms

Previously the potential for spin-correlated radical pairs (SCRPs) to be used as molecular qubits for quantum sensing²²⁴ has been recognized and covered in a comprehensive review²⁵. Here we will summarize some of the key

points, elaborate on connections with CISS in radical pair systems, and finalize with a discussion on prospects for SCRPs generated in donor-chiral bridge-acceptor molecules as an emerging platform for quantum information and sensing.

In the previous section we described several sensing platforms that make use of the CISS effect. Following the classifications of Degen *et al.*²²⁵, most of these predominantly fall under the category of type-I sensors, which make use of a quantum system to measure a classical or quantum physical quantity. However, there is potential scope for type-II sensors, that make use of quantum coherence to measure a quantity, or type-III sensors that make use of entanglement to improve the sensitivity or precision of measurement beyond what is classically possible. In particular, SCRPs have a few desirable properties in which coherent singlet-triplet interconversion can last up to 100 ns and potentially up to microsecond timescales in radical pairs relevant to magnetoreception^{226–230}. This makes them promising candidates for quantum sensing applications and beyond. For example, Xie *et al.*²²⁴ used a photogenerated SCRP formed from a radical ion pair to sense an electric field change created at one radical ion of the pair using molecular recognition. Using pulse-EPR measurements of oscillations caused by the distance dependent electron-electron dipolar coupling to analyze the distance between the two spins of the SCRP. Although SCRPs have currently been limited to type-I and type-II sensors, given that they constitute molecules that have unpaired electron spins that can be generated in pure quantum states, there is a potential to make use of quantum properties such as entanglement and efforts underway to make use of them as spin qubit pairs. Beyond this, Lin & Mani²³¹ have explored their use in amplifying magnetic field effects via triplet-triplet annihilation and the Wasielewski group has made progress into the application of SCRPs in quantum information and communication protocols^{189,232–235}, and has reviewed the trajectory to these applications from photosynthetic energy transduction and biomimetics.

On the topic of attaining inspiration from biochemical design principles, and optimizing these in new technologies, SCRPs have been studied heavily in the context of the spin biochemistry of magnetoreception. Quantum phenomena, such as quantum coherence and superposition, are generally not expected to survive in noisy ambient conditions, and so it is of interest to identify if nature has found ways to protect quantum resources in biological settings²³⁶. Fay *et al.* have identified the radical pair requires full quantum mechanical calculations for an accurate description, suggesting that quantum effects may play an important role²³⁷. Moreover, investigations into radical pair-based magnetosensitivity may provide useful insights and tools for SCRP applications, such as elucidating the utilitarian role of quantum resources^{238–242}, quantum limit frameworks to assess quantum sensing capabilities^{243–246}, quantum control of SCRPs^{247–250}, and enhancement mechanisms for magnetic field sensitivity and coherence, e.g. through spin relaxation^{251,252}, radical motion^{253,254}, three-radical mechanisms^{255–257}, and the quantum Zeno effect^{188,258,259}.

Attention has also turned to the potential role of CISS in

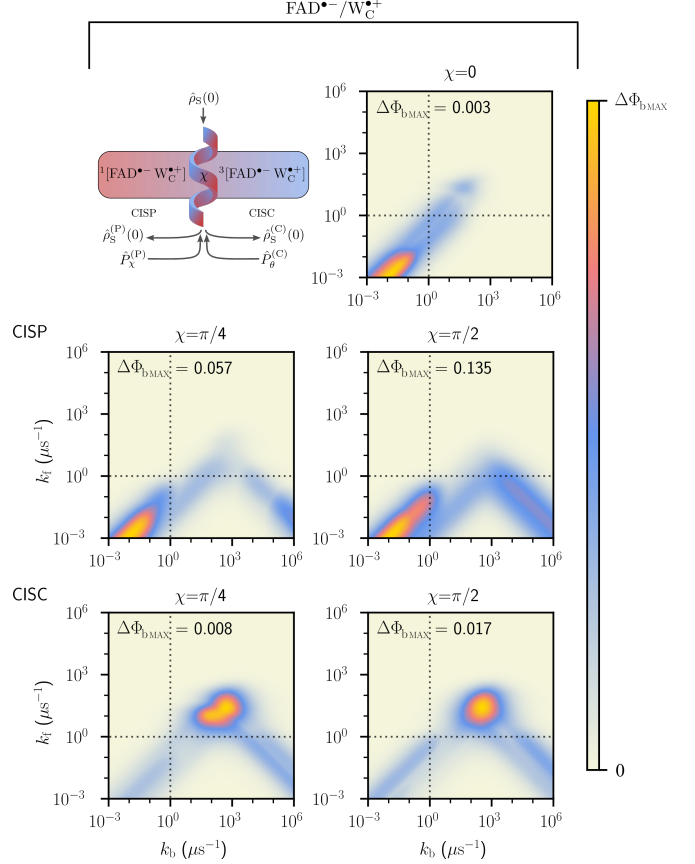


FIG. 23. CISS modulated magnetic field sensitivity for the flavin-tryptophan ($\text{FAD}^{\bullet-}/\text{W}_C^{\bullet+}$) radical pair system. Heatmaps show the sensitivity as assessed by the difference in recombination yields ($\Delta\Phi_b$) sampled over 300 magnetic field orientations and 200×200 combinations of recombination k_b and forward reaction k_f rates, under Zeeman, hyperfine, and electron-electron dipolar interactions. The case of no CISS effects $\chi = 0$, is compared to varying degrees of CISS $\chi = \pi/4$ and $\chi = \pi/2$ for both chirality induced spin polarization (CISP) and chirality induced spin coherence (CISC) models. Significant sensitivities are produced for asymmetric recombination, indicative of the quantum Zeno effect, only if polarization is generated. Dotted lines denote conventional parameter choices of reaction rates at $1\mu\text{s}^{-1}$. Adapted with permission from Smith *et al.*¹⁸⁸, arXiv:2505.01519 (2025). Copyright 2025 Authors, licensed under a Creative Commons Attribution (CC BY) license.

magnetoreception where, following on from the framework by Luo & Hore¹⁷⁹ introduced in Sec. III G, it has been predicted by Tiwari & Poonia^{180,181} to enhance SCRP sensitivity to magnetic fields, and coherence. The exact mechanism behind these enhancements was unknown, but the most prominent enhancements emerged at strongly asymmetric recombination regimes of the radical pair. Following this, Smith *et al.*¹⁸⁸ investigated both singlet-born and triplet-born radical pairs implicated in biological magnetosensing for models of CISS that are selective for polarization or only coherence. They found that CISS-generated spin polarization significantly enhances magnetic field sensitivity by introducing triplet character into the initial state and reinforcing the quan-

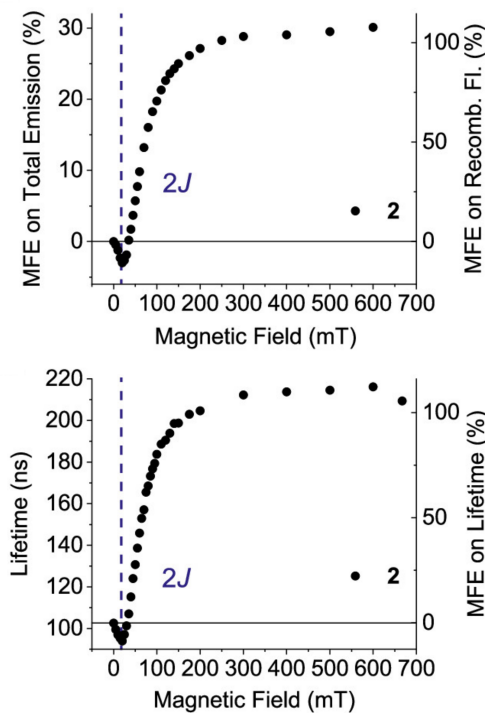


FIG. 24. Magnetic modulation of optical properties of a donor-chiral bridge-acceptor molecule. The top plot shows magnetic field effects (MFEs) on total emission (left axis) and recombination fluorescence only (right axis), measured relative to a null field (MFE (%)) = $\frac{I(B=ON)}{I(B=OFF)} - 1 \times 100$, where I is the intensity of emission. The bottom plot shows magnetic modulation of the recombination fluorescence time (left axis) and its MFEs (right axis) (MFE (%)) = $\frac{\tau(B=ON)}{\tau(B=OFF)} - 1 \times 100$, where τ is the lifetime. Adapted with permission from Lin *et al.*²², J. Am. Chem. Soc. **147**, 11062–11071 (2025). Copyright 2025 American Chemical Society.

tum Zeno effect, which operates at strongly asymmetric recombination rates, while CISS-generated spin coherence was less effective at providing enhancements (Fig. 23). This highlights that CISS in itself is not a universal enhancer of sensitivity or coherence, but should be evaluated alongside the quantum Zeno effect in cryptochromes radical pairs, and that the role of generating polarization effects through an incoherent process, could be essential beyond fundamental importance to practical function of CISS in SCRPs. Although the functionality of CISS and SCRPs in biological processes remains an open question, these investigations may help to guide the biomimetic engineering of molecular quantum sensors.

Recently, Lin *et al.*²² introduced an emerging platform based on donor-chiral bridge-acceptor (D- χ -A) molecules that boast significant magnetic field effects (MFEs) on fluorescence intensity and SCRP lifetimes, even in solution at ambient conditions. These systems build upon previous designs by the Mani group for donor-bridge-acceptor (D-B-A) molecules for optical readout of magnetic-field-sensitive SCRPs at room temperature. While the reported changes for those systems were modest, the D- χ -A design exhibit significant magnetic

field effects on recombination fluorescence, where the chiral bridge provides sufficient electronic couplings to ensure long-lived SCRPs. Although the role of CISS was not explicitly resolved by Lin *et al.*, similar chiral-bridged molecules have been used to investigate and demonstrate the CISS effect, giving credence to the plausibility that CISS could contribute in these systems^{39,260}. The advantage of molecular synthetic control, was demonstrated through three structural modifications to the donor site via distance extension, torsional locking, and planarization. These changes produced an observed magnetic sensitivity increase of > 200% in emission lifetimes, with up to 30% modulation of total emission intensity (Fig. 24). Furthermore, as these structural changes allow the system rigidity and donor-acceptor distance to be altered, and spin relaxation via singlet-triplet dephasing mechanisms to be modulated, it is plausible that some of the enhancement and control schemes identified in biological SCRPs could be implemented^{249,261,262}.

D- χ -A SCRPs represent a promising emerging platform of SCRP-based molecular quantum sensors²⁶³, with the potential to extend beyond classical sensing capabilities to address a wide range of applications from biological to condensed matter systems^{264–266}. Their long-lived spin coherence, room-temperature operation, optical addressability, and structural tunability positions them as strong candidates for developing type-II and type-III quantum sensors that exploit quantum resources such as quantum coherence and entanglement. Moreover, these systems offer a complementary perspective by not only acting as sensors, but also providing testbeds, alongside NV-based quantum sensing to probe fundamental questions about quantum properties of radical pairs and the role of CISS^{53,267,268}.

V. CONCLUDING REMARKS

CISS has given rise to a rich landscape of experimental findings and promising application since its inception. Though the sheer breadth of CISS studies may obscure the key mechanisms underlying the effect for new entrants, we attempt to lay out a clearer picture of the cumulative efforts into clarifying its origins in an effort to portray a broader point-of-view through which debated issues around CISS may be demystified. At its essence, CISS arises from chiral geometry where finite spin-orbit coupling arises. This generates a spin-texture in reciprocal-space, which gives rise to spin-current when a bias is applied or when charge-current is finite. In an ideal chiral object, this spin-current is entirely non-dissipative and results only in the generation of a magnetic order in the molecule. This is possible because the chiral anomaly breaks conservation of quantized spin-current, contrary to classical-leaning intuitions built on charge-current characteristics.

Naturally, no CISS emerges in equilibrium as no spin-current appears in the absence of external perturbations or applied fields; but it is noteworthy that neither bias alone nor a reversed external magnetic field is sufficient for the *observation* of CISS-transport through biomolecular junctions due to

its reliance on magnetocurrent anisotropy as an index of spin-selectivity. This requires both a finite dissipative spin-current and the additional disruption of Onsager-Casimir relations, which may be fulfilled when external dissipation of the system or dephasing is introduced (a core source of investigation from Guo & Sun⁸⁵ to Fransson⁸⁶), or when the setup is simply complicated enough to reasonably discard ideal assumptions. In practice, this is likely to be the case: since bias or charge-current gives rise to a monopole-like spin texture in the chiral object, such a chiral object in quasi-equilibrium is effectively (partially-)ferromagnetised, which contributes to the rich interfacial effects prevalent in CISS experiments. The latter point also accounts for differences in response between CISS in biomolecules (arguably, the ‘canonical form’ of CISS) and CISS in non-doped crystals/metals: even in the absence of bias, wavefunction penetration of a substrate into a chiral bridge can alter electronic properties of the system and give rise to magnetisation-dependent charge-trapping effects in the presence of defect-sites⁸⁷. This dichotomy between dissipation and coherence is featured in other realisations of CISS beyond the realm of molecular junctions: Fay & Limmer’s¹⁸⁵ SCRP model suggests that spin-orbit coupling gives rise to singlet-triplet coherences which can only then be converted to spin-selectivity by an incoherent electron-transfer step, a finding significant for characterizing enhancements to sensitivity and spin-coherence generation using CISS. Consequently, this may go beyond fundamental interest, to be of essential importance in the development of CISS enabled SCRP-based quantum sensors and may carry across to other CISS based sensing and quantum information applications.

Additionally, it is interesting to see how CISS may be tethered to broader perspectives on chirality: a topological perspective, for instance, shows how gapless Kramers-Weyl fermions naturally appear that are protected by the *lack* of structural inversion-symmetry; and the emergence of entanglement in the ground-state structure thereof make chiral-crystalline materials prime ground for functional quantum effects. A century ago, the first theoretical frameworks for quantum mechanics and electron spin^{269,270} arose in part as a response to the lack of understanding and consensus in regards to anomalies in spectroscopy. So while much remains yet unclear as to CISS’s relation to other notions of chirality across different fields; it is an interesting open theoretical question whether some deeper underlying principle, that connects chirality with spin-selectivity, would help us better confront the uneasy gap that currently exists between the formalisms we have and the phenomena we observe across realisations of CISS. Whether this potentially happens to already be utilized by nature is also an open matter at this time.

VI. ACKNOWLEDGEMENTS

Y.X.F. acknowledges support from the CNYSP Office at the Nanyang Technological University, Singapore, toward a research visit with the QuBiT Lab at the University of California, Los Angeles. A.K. acknowledges support from an NSF GRFP. F.T.C. and L.D.S. acknowledge support from the Of-

fice of Naval Research (ONR Award No. N62909-21-1-2018) and the Engineering and Physical Sciences Research Council (EP/X027376/1). For the purpose of open access, the authors have applied a Creative Commons Attribution (CC BY) license to any Author Accepted Manuscript version arising from this submission.

AUTHOR DECLARATIONS

Conflict of interest

The authors have no conflicts to disclose.

DATA AVAILABILITY STATEMENT

Data sharing is not applicable to this article as no new data were created or analyzed in this study.

- ¹C. S. Wu, E. Ambler, R. W. Hayward, D. D. Hoppes, and R. P. Hudson, “Experimental test of parity conservation in beta decay,” Phys. Rev. **105**, 1413–1415 (1957).
- ²N. Vargesson, “Thalidomide-induced teratogenesis: History and mechanisms,” Birth Defects Research Part C: Embryo Today: Reviews **105**, 140–156 (2015).
- ³L. A. Nguyen, H. He, and C. Pham-Huy, “Chiral Drugs: An Overview,” Int. J. Biomed. Sci. **2**, 85 (2006).
- ⁴M. Liu, L. Zhang, and T. Wang, “Supramolecular Chirality in Self-Assembled Systems,” Chem. Rev **115**, 7304–7397 (2015).
- ⁵D. G. Blackmond, “The Origin of Biological Homochirality,” Cold Spring Harb. Perspect. Biol. **11**, a032540 (2019).
- ⁶Y. Chen and W. Ma, “The origin of biological homochirality along with the origin of life,” PLoS Comput. Biol. **16**, e1007592 (2020).
- ⁷S. F. Ozturk, Z. Liu, J. D. Sutherland, and D. D. Sasselov, “Origin of biological homochirality by crystallization of an RNA precursor on a magnetic surface,” Sci. Adv. **9**, eadg8274 (2023).
- ⁸D. P. Glavin, A. S. Burton, J. E. Elsila, J. C. Aponte, and J. P. Dworkin, “The Search for Chiral Asymmetry as a Potential Biosignature in our Solar System,” Chem. Rev **120**, 4660–4689 (2020).
- ⁹S. F. Ozturk, D. D. Sasselov, and J. D. Sutherland, “The central dogma of biological homochirality: How does chiral information propagate in a prebiotic network?” J. Chem. Phys. **159**, 061102 (2023).
- ¹⁰M. Briggeman *et al.*, “Engineered chirality of one-dimensional nanowires,” Sci. Adv. **11**, eadx4761 (2025).
- ¹¹N. C. Bradbury, T. Duston, Z. Tao, J. I. Rawlinson, R. Littlejohn, and J. Subotnik, “Symmetry breaking as predicted by a phase space hamiltonian with a spin coriolis potential,” Journal Chem. Phys. **162**, 244107 (2025).
- ¹²A. Aharony and O. Entin-Wohlman, “Spin-orbit interactions, time-reversal symmetry, and spin selection,” J. Chem. Phys. **162**, 154103 (2025).
- ¹³S. Mohtashim, A. Das, T. Chatterjee, and F. T. Chowdhury, “A near-term quantum simulation of the transverse field ising model hints at glassy dynamics,” Eur. Phys. J. Spec. Top. (2025), 10.1140/epjs/s11734-025-01630-y.
- ¹⁴S. Sadhukhan, S. Dey, S. Karmakar, and S. K. Nandi, “A perspective on active glassy dynamics in biological systems,” Eur. Phys. J. Spec. Top. (2024), 10.1140/epjs/s11734-024-01188-1.
- ¹⁵J. Fransson, “Charge and Spin Dynamics and Enantioselectivity in Chiral Molecules,” J. Phys. Chem. Lett. **13**, 808–814 (2022).
- ¹⁶A. Shitade and E. Minamitani, “Geometric spin-orbit coupling and chirality-induced spin selectivity,” New J. Phys. **22**, 113023 (2020).
- ¹⁷K. Ray, S. P. Ananthavel, D. H. Waldeck, and R. Naaman, “Asymmetric Scattering of Polarized Electrons by Organized Organic Films of Chiral Molecules,” Science **283**, 814–816 (1999).

- ¹⁸S. Mayer and J. Kessler, "Experimental verification of electron optic dichroism," *Phys. Rev. Lett.* **74**, 4803–4806 (1995).
- ¹⁹C. Nolting, S. Mayer, and J. Kessler, "Electron dichroism - new data and an experimental cross-check," *J. Phys. B: At. Mol. Opt. Phys.* **30**, 5491 (1997).
- ²⁰Y. Sang *et al.*, "Temperature Dependence of Charge and Spin Transfer in Azurin," *J. Phys. Chem. C* **125**, 9875–9883 (2021).
- ²¹T. K. Das, F. Tassinari, R. Naaman, and J. Fransson, "Temperature-Dependent Chiral-Induced Spin Selectivity Effect: Experiments and Theory," *J. Phys. Chem. C* **126**, 3257–3264 (2022).
- ²²N. Lin *et al.*, "Molecular engineering of emissive molecular qubits based on spin-correlated radical pairs," *J. Am. Chem. Soc.* **147**, 11062–11071 (2025).
- ²³S. K. Kuppusamy, D. Hunger, M. Ruben, P. Goldner, and D. Serrano, "Spin-bearing molecules as optically addressable platforms for quantum technologies," *Nanophotonics* **13**, 4357–4379 (2024).
- ²⁴J. J. Zakrzewski, M. Liberka, J. Wang, S. Chorazy, and S.-i. Ohkoshi, "Optical phenomena in molecule-based magnetic materials," *Chem. Rev.* **124**, 5930–6050 (2024).
- ²⁵T. Mani, "Molecular qubits based on photogenerated spin-correlated radical pairs for quantum sensing," *Chem. Phys. Rev.* **3**, 021301 (2022).
- ²⁶C. D. Aiello *et al.*, "A chirality-based quantum leap," *ACS Nano* **16**, 4989–5035 (2022).
- ²⁷S. Vizvary, A. Valdes-Curiel, C. Aiello, and L. Ginsberg, "Quantum sensing in a warm, noisy environment: Understanding spin-mediated effects in biological materials," *Bull. Am. Phys. Soc.* (2024).
- ²⁸H. Lee, N. Yang, and A. E. Cohen, "Mapping nanomagnetic fields using a radical pair reaction," *Nano Lett.* **11**, 5367–5372 (2011).
- ²⁹A. C. Aragonès *et al.*, "Measuring the spin-polarization power of a single chiral molecule," *Small* **13**, 1602519 (2017).
- ³⁰M. R. Safari, F. Matthes, C. M. Schneider, K.-H. Ernst, and D. E. Bürgler, "Spin-selective electron transport through single chiral molecules," *Small* **20**, 2308233 (2024).
- ³¹A. M. Ortúñoz *et al.*, "Chiral single-molecule potentiometers based on stapled ortho- oligo(phenylene)ethynlenes," *Angew. Chem. Int. Ed.* **62**, e202218640 (2023).
- ³²A. Kumar, E. Capua, M. K. Kesharwani, J. M. L. Martin, E. Sitbon, D. H. Waldeck, and R. Naaman, "Chirality-induced spin polarization places symmetry constraints on biomolecular interactions," *Proc. Natl. Acad. Sci.* **114**, 2474–2478 (2017).
- ³³O. Ben Dor *et al.*, "Magnetization switching in ferromagnets by adsorbed chiral molecules without current or external magnetic field," *Nat. Commun.* **8**, 14567 (2017).
- ³⁴I. Meirzada *et al.*, "Long-Time-Scale Magnetization Ordering Induced by an Adsorbed Chiral Monolayer on Ferromagnets," *ACS Nano* **15**, 5574–5579 (2021).
- ³⁵T. Liu *et al.*, "Chirality-induced magnet-free spin generation in a semiconductor," *Adv. Mater.* **36**, 2406347 (2024).
- ³⁶A. Moharana *et al.*, "Chiral-induced unidirectional spin-to-charge conversion," *Sci. Adv.* **11**, eado4285 (2025).
- ³⁷R. A. Rosenberg, D. Mishra, and R. Naaman, "Chiral selective chemistry induced by natural selection of spin-polarized electrons," *Angew. Chem. Int. Ed.* **54**, 7295–7298 (2015).
- ³⁸J. M. Abendroth, K. M. Cheung, D. M. Stemmer, M. S. El Hadri, C. Zhao, E. E. Fullerton, and P. S. Weiss, "Spin-Dependent Ionization of Chiral Molecular Films," *J. Am. Chem. Soc.* **141**, 3863–3874 (2019).
- ³⁹H. J. Eckvahl *et al.*, "Direct observation of chirality-induced spin selectivity in electron donor–acceptor molecules," *Science* **382**, 197–201 (2023).
- ⁴⁰A. K. Mondal *et al.*, "Spin Filtering in Supramolecular Polymers Assembled from Achiral Monomers Mediated by Chiral Solvents," *J. Am. Chem. Soc.* **143**, 7189–7195 (2021).
- ⁴¹S. Pandey *et al.*, "Chirality transmission in macromolecular domains," *Nat. Commun.* **13**, 76 (2022).
- ⁴²K. Banerjee-Ghosh *et al.*, "Separation of enantiomers by their enantiospecific interaction with achiral magnetic substrates," *Science* **360**, 1331–1334 (2018).
- ⁴³K. Banerjee-Ghosh, S. Ghosh, H. Mazal, I. Riven, G. Haran, and R. Naaman, "Long-range charge reorganization as an allosteric control signal in proteins," *J. Am. Chem. Soc.* **142**, 20456–20462 (2020).
- ⁴⁴T. S. Metzger *et al.*, "The electron spin as a chiral reagent," *Angew. Chem. Int. Ed.* **59**, 1653–1658 (2020).
- ⁴⁵W. Mtangi *et al.*, "Control of electrons' spin eliminates hydrogen peroxide formation during water splitting," *J. Am. Chem. Soc.* **139**, 2794–2798 (2017).
- ⁴⁶W. Zhang, K. Banerjee-Ghosh, F. Tassinari, and R. Naaman, "Enhanced electrochemical water splitting with chiral molecule-coated Fe₃O₄ nanoparticles," *ACS Energy Lett.* **3**, 2308–2313 (2018).
- ⁴⁷Y.-H. Kim *et al.*, "Chiral-induced spin selectivity enables a room-temperature spin light-emitting diode," *Science* **371**, 1129–1133 (2021).
- ⁴⁸S. He *et al.*, "Perovskite spin light-emitting diodes with simultaneously high electroluminescence dissymmetry and high external quantum efficiency," *Nat. Commun.* **16** (2025), 10.1038/s41467-025-57472-8.
- ⁴⁹R. Pan, K. Wang, and Z.-G. Yu, "Magnetic-field manipulation of circularly polarized photoluminescence in chiral perovskites," *Mater. Horiz.* **9**, 740–747 (2022).
- ⁵⁰Y. Li *et al.*, "Unraveling chiral perovskite spin-light emitting diode performance and magneto-chiroptical properties relationship due to the synergistic effect," *Adv. Funct. Mater.* **n/a**, 2424619 (2025).
- ⁵¹G. Zhang *et al.*, "High-performance sky-blue perovskite spin-light emitting diodes due to chiral ionic liquid implantation and passivation," *Adv. Funct. Mater.* **n/a**, 2503088 (2025).
- ⁵²J. Tang *et al.*, "Chiral ionic liquids enable high-performance room temperature single junction spin-light emitting diodes," *Laser Photonics Rev.* **19**, 2401008 (2025).
- ⁵³L. A. Völker, K. Herb, E. Janitz, C. L. Degen, and J. M. Abendroth, "Toward quantum sensing of chiral induced spin selectivity: Probing donor–bridge–acceptor molecules with nv centers in diamond," *J. Chem. Phys.* **158**, 161103 (2023).
- ⁵⁴N. Giacconi *et al.*, "Efficient spin-selective electron transport at low voltages of thia-bridged triarylamine hetero[4]helicenes chemisorbed monolayer," *ACS Nano* **17**, 15189–15198 (2023).
- ⁵⁵N. Bangruwa, P. k. Bhartiya, and D. Mishra, "A novel spin-based label-free electrochemical DNA hybridization biosensor and its applications for dengue virus detection," *Sens. Actuators B Chem.* **382**, 133447 (2023).
- ⁵⁶E. Pyurbeeva, J. O. Thomas, and J. A. Mol, "Non-equilibrium thermodynamics in a single-molecule quantum system," *Mater. Quantum Technol.* **3**, 025003 (2023).
- ⁵⁷R. Naaman, Y. Paltiel, and D. H. Waldeck, "Chiral Molecules and the Spin Selectivity Effect," *J. Phys. Chem. Lett.* **11**, 3660–3666 (2020).
- ⁵⁸R. Naaman and D. H. Waldeck, "Chiral-induced spin selectivity effect," *J. Phys. Chem. Lett.* **3**, 2178–2187 (2012).
- ⁵⁹R. Naaman and D. H. Waldeck, "Spintronics and chirality: Spin selectivity in electron transport through chiral molecules," *Annu. Rev. Phys. Chem.* **66**, 263–281 (2015).
- ⁶⁰K. Michaeli, V. Varade, R. Naaman, and D. H. Waldeck, "A new approach towards spintronics–spintronics with no magnets," *J. Phys.: Condens. Matter* **29**, 103002 (2017).
- ⁶¹S. Alwan and Y. Dubi, "Spinterface Origin for the Chirality-Induced Spin-Selectivity Effect," *J. Am. Chem. Soc.* **143**, 14235–14241 (2021).
- ⁶²Y. Dubi, "Spinterface chirality-induced spin selectivity effect in biomolecules," *Chem. Sci.* **13**, 10878–10883 (2022).
- ⁶³B. P. Bloom, Y. Paltiel, R. Naaman, and D. H. Waldeck, "Chiral Induced Spin Selectivity," *Chem. Rev.* **124**, 1950–1991 (2024).
- ⁶⁴J. Boeyens, J. Glathard, E. Gandar, S. Nimmrichter, L. A. Correa, and J. Rubio, "On the role of symmetry and geometry in global quantum sensing," *arXiv:2502.14817* (2025).
- ⁶⁵A. Y. Lee *et al.*, "Tunable spin qubit pairs in quantum dot–molecule conjugates," *ACS Nano* **19**, 12194–12207 (2025).
- ⁶⁶A. Chiesa *et al.*, "Chirality-induced spin selectivity at the molecular level: A different perspective to understand and exploit the phenomenon," *J. Phys. Chem. Lett.* **16**, 5358–5372 (2025).
- ⁶⁷I. Carmeli, K. S. Kumar, O. Heifler, C. Carmeli, and R. Naaman, "Spin Selectivity in Electron Transfer in Photosystem I," *Angew. Chem. Int. Ed.* **53**, 8953–8958 (2014).
- ⁶⁸S. Alwan, S. Sarkar, A. Sharoni, and Y. Dubi, "Temperature-dependence of the chirality-induced spin selectivity effect—Experiments and theory," *J. Chem. Phys.* **159**, 014106 (2023).
- ⁶⁹J. Fransson, "The Chiral Induced Spin Selectivity Effect: What It Is, What It Is Not, And Why It Matters," *Isr. J. Chem.* **62**, e202200046 (2022).

- ⁷⁰Y. Liu, J. Xiao, J. Koo, and B. Yan, "Chirality-driven topological electronic structure of DNA-like materials," *Nat. Mat.* **20**, 638–644 (2021).
- ⁷¹J. H. Bardarson, "A proof of the kramers degeneracy of transmission eigenvalues from antisymmetry of the scattering matrix," *J. Phys. A: Math. Theor.* **41**, 405203 (2008).
- ⁷²Y. Utsumi, T. Kato, O. Entin-Wohlman, and A. Aharony, "Spin-filtering in a p-orbital helical atomic chain," *Isr. J. Chem.* **62**, e202200107 (2022).
- ⁷³Y. Utsumi, O. Entin-Wohlman, and A. Aharony, "Spin selectivity through time-reversal symmetric helical junctions," *Phys. Rev. B* **102**, 035445 (2020).
- ⁷⁴Y. Wolf *et al.*, "Unusual Spin Polarization in the Chirality-Induced Spin Selectivity," *ACS Nano* **16**, 18601–18607 (2022).
- ⁷⁵X. Yang, C. H. van der Wal, and B. J. van Wees, "Spin-dependent electron transmission model for chiral molecules in mesoscopic devices," *Phys. Rev. B* **99**, 024418 (2019).
- ⁷⁶X. Yang, C. H. van der Wal, and B. J. van Wees, "Reply to "Comment on "Spin-dependent electron transmission model for chiral molecules in mesoscopic devices""," *Phys. Rev. B* **101**, 026404 (2020).
- ⁷⁷S. Varela *et al.*, "Spin-orbit interaction and spin selectivity for tunneling electron transfer in DNA," *Phys. Rev. B* **101**, 241410 (2020).
- ⁷⁸K. Michaeli and R. Naaman, "Origin of Spin-Dependent Tunneling Through Chiral Molecules," *J. Phys. Chem. C* **123**, 17043–17048 (2019).
- ⁷⁹A. Ghazaryan, Y. Paltiel, and M. Lemeshko, "Analytic Model of Chiral-Induced Spin Selectivity," *J. Phys. Chem. C* **124**, 11716–11721 (2020).
- ⁸⁰O. Entin-Wohlman, A. Aharony, and Y. Utsumi, "Comment on "spin-orbit interaction and spin selectivity for tunneling electron transfer in DNA","" *Phys. Rev. B* **103**, 077401 (2021).
- ⁸¹J. Fröhlich and U. M. Studer, "Gauge invariance and current algebra in nonrelativistic many-body theory," *Rev. Mod. Phys.* **65**, 733–802 (1993).
- ⁸²I. V. Tokatly, "Equilibrium spin currents: Non-abelian gauge invariance and color diamagnetism in condensed matter," *Phys. Rev. Lett.* **101**, 106601 (2008).
- ⁸³R. Gebauer and R. Car, "Kinetic theory of quantum transport at the nanoscale," *Phys. Rev. B* **70**, 125324 (2004).
- ⁸⁴M. S. Zöllner *et al.*, "Insight into the Origin of Chiral-Induced Spin Selectivity from a Symmetry Analysis of Electronic Transmission," *J. Chem. Theory Comput.* **16**, 2914–2929 (2020).
- ⁸⁵A.-M. Guo and Q.-F. Sun, "Spin-dependent electron transport in protein-like single-helical molecules," *Proc. Natl. Acad. Sci.* **111**, 11658–11662 (2014).
- ⁸⁶J. Fransson, "Chiral induced spin polarized electron current: Origin of the chiral induced spin selectivity effect," *J. Phys. Chem. Lett.* **16**, 4346–4353 (2025).
- ⁸⁷Y. Zhao, K. Zhang, J. Xiao, K. Sun, and B. Yan, "Magnetochemical charge pumping due to charge trapping and skin effect in chirality-induced spin selectivity," *Nat. Commun.* **16**, 37 (2025).
- ⁸⁸R. Sun *et al.*, "Colossal anisotropic absorption of spin currents induced by chirality," *Sci. Adv.* **10**, eadn3240 (2024).
- ⁸⁹E. Díaz, A. Contreras, J. Hernández, and F. Domínguez-Adame, "Effective nonlinear model for electron transport in deformable helical molecules," *Phys. Rev. E* **98**, 052221 (2018).
- ⁹⁰S. Dalum and P. Hedegård, "Theory of Chiral Induced Spin Selectivity," *Nano Lett.* **19**, 5253–5259 (2019).
- ⁹¹T. Liu *et al.*, "Linear and Nonlinear Two-Terminal Spin-Valve Effect from Chirality-Induced Spin Selectivity," *ACS Nano* **14**, 15983–15991 (2020).
- ⁹²R. Gupta and A. Droghetti, "Current-induced spin polarization in chiral tellurium: A first-principles quantum transport study," *Phys. Rev. B* **109**, 155141 (2024).
- ⁹³X. Yang and B. J. van Wees, "Linear-response magnetoresistance effects in chiral systems," *Phys. Rev. B* **104**, 155420 (2021).
- ⁹⁴K. Shiota *et al.*, "Chirality-induced spin polarization over macroscopic distances in chiral disilicide crystals," *Phys. Rev. Lett.* **127**, 126602 (2021).
- ⁹⁵A. Inui *et al.*, "Chirality-induced spin-polarized state of a chiral crystal crnb_3s_6 ," *Phys. Rev. Lett.* **124**, 166602 (2020).
- ⁹⁶S.-W. Cheong and X. Xu, "Magnetic chirality," *npj Quantum Mater.* **7**, 40 (2022).
- ⁹⁷C. Kulkarni *et al.*, "Highly Efficient and Tunable Filtering of Electrons' Spin by Supramolecular Chirality of Nanofiber-Based Materials," *Adv. Mater.* **32**, 1904965 (2020).
- ⁹⁸M. Eckshtain-Levi *et al.*, "Cold denaturation induces inversion of dipole and spin transfer in chiral peptide monolayers," *Nat. Commun.* **7**, 10744 (2016).
- ⁹⁹G. Wagner *et al.*, "Probing chiral symmetry with a topological domain wall sensor," *Newton* (2025).
- ¹⁰⁰P. D. Sacramento and M. F. Madeira, "Topological states in chiral electronic chains," *Phys. Rev. B* **106**, 085130 (2022).
- ¹⁰¹J. Gersten, K. Kaasbjerg, and A. Nitzan, "Induced spin filtering in electron transmission through chiral molecular layers adsorbed on metals with strong spin-orbit coupling," *J. Chem. Phys.* **139**, 114111 (2013).
- ¹⁰²L. Li *et al.*, "Too fast for spin flipping: Absence of chirality-induced spin selectivity in coherent electron transport through single-molecule junctions," *J. Am. Chem. Soc.* **147**, 25043–25051 (2025).
- ¹⁰³G. Chang *et al.*, "Topological quantum properties of chiral crystals," *Nat. Mat.* **17**, 978–985 (2018).
- ¹⁰⁴P. Hosur, X. Dai, Z. Fang, and X.-L. Qi, "Time-reversal-invariant topological superconductivity in doped weyl semimetals," *Phys. Rev. B* **90**, 045130 (2014).
- ¹⁰⁵Y. Adhikari *et al.*, "Interplay of structural chirality, electron spin and topological orbital in chiral molecular spin valves," *Nat. Commun.* **14**, 5163 (2023).
- ¹⁰⁶V. F. Kershaw and D. S. Kosov, "Nonequilibrium green's function theory for nonadiabatic effects in quantum electron transport," *J. Chem. Phys.* **147**, 224109 (2017).
- ¹⁰⁷V. F. Kershaw and D. S. Kosov, "Non-adiabatic effects of nuclear motion in quantum transport of electrons: A self-consistent keldysh-langevin study," *J. Chem. Phys.* **153**, 154101 (2020).
- ¹⁰⁸X. Bian *et al.*, "Modeling nonadiabatic dynamics with degenerate electronic states, intersystem crossing, and spin separation: A key goal for chemical physics," *J. Chem. Phys.* **154**, 110901 (2021).
- ¹⁰⁹X. Bian, T. Qiu, J. Chen, and J. E. Subotnik, "On the meaning of Berry force for unrestricted systems treated with mean-field electronic structure," *J. Chem. Phys.* **156**, 234107 (2022).
- ¹¹⁰D. Suárez-Forero, M. Jalali Mehrabad, C. Vega, A. González-Tudela, and M. Hafezi, "Chiral quantum optics: Recent developments and future directions," *PRX Quantum* **6**, 020101 (2025).
- ¹¹¹B. Göhler *et al.*, "Spin Selectivity in Electron Transmission Through Self-Assembled Monolayers of Double-Stranded DNA," *Science* **331**, 894–897 (2011).
- ¹¹²I. Katsantonis *et al.*, "Giant enhancement of nonreciprocity in gyrotrropic heterostructures," *Sci. Rep.* **13**, 21986 (2023).
- ¹¹³S. S. Andrews and J. Tretton, "Physical Principles of Circular Dichroism," *Journal of Chemical Education* **97**, 4370–4376 (2020).
- ¹¹⁴S. Yeganeh, M. A. Ratner, E. Medina, and V. Mujica, "Chiral electron transport: Scattering through helical potentials," *J. Chem. Phys.* **131**, 014707 (2009).
- ¹¹⁵E. Medina, F. López, M. A. Ratner, and V. Mujica, "Chiral molecular films as electron polarizers and polarization modulators," *Europhys. Lett.* **99**, 17006 (2012).
- ¹¹⁶S. Varela, E. Medina, F. López, and V. Mujica, "Inelastic electron scattering from a helical potential: transverse polarization and the structure factor in the single scattering approximation," *J. Phys.: Condens. Matter* **26**, 015008 (2013).
- ¹¹⁷M. Kettner *et al.*, "Chirality-Dependent Electron Spin Filtering by Molecular Monolayers of Helicenes," *J. Phys. Chem. Lett.* **9**, 2025–2030 (2018).
- ¹¹⁸W. Xu, A. A. Bagrov, F. T. Chowdhury, L. D. Smith, D. R. Kattnig, H. J. Kappen, and M. I. Katsnelson, "Fröhlich versus bose-einstein condensation in pumped bosonic systems," *Phys. Rev. Res.* **7**, 023111 (2025).
- ¹¹⁹R. C. T. da Costa, "Quantum mechanics of a constrained particle," *Phys. Rev. A* **23**, 1982–1987 (1981).
- ¹²⁰R. Gutierrez *et al.*, "Modeling Spin Transport in Helical Fields: Derivation of an Effective Low-Dimensional Hamiltonian," *J. Phys. Chem. C* **117**, 22276–22284 (2013).
- ¹²¹M. Geyer, R. Gutierrez, and G. Cuniberti, "Effective Hamiltonian model for helically constrained quantum systems within adiabatic perturbation theory: Application to the chirality-induced spin selectivity (CISS) effect," *J. Chem. Phys.* **152**, 214105 (2020).
- ¹²²S. Campbell *et al.*, "Roadmap on quantum thermodynamics," arXiv:2504.20145 (2025).

- ¹²³B. Mashhoon, "Neutron interferometry in a rotating frame of reference," *Phys. Rev. Lett.* **61**, 2639–2642 (1988).
- ¹²⁴M. Matsuo, J. Ieda, E. Saitoh, and S. Maekawa, "Spin-dependent inertial force and spin current in accelerating systems," *Phys. Rev. B* **84**, 104410 (2011).
- ¹²⁵M. Matsuo, J. Ieda, E. Saitoh, and S. Maekawa, "Effects of Mechanical Rotation on Spin Currents," *Phys. Rev. Lett.* **106**, 076601 (2011).
- ¹²⁶R. Shekhter, O. Entin-Wohlman, M. Jonson, and A. Aharonov, "Magnetoconductance Anisotropies and Aharonov-Casher Phases," *Phys. Rev. Lett.* **129**, 037704 (2022).
- ¹²⁷D. Nürenberg and H. Zacharias, "Evaluation of spin-flip scattering in chirality-induced spin selectivity using the Riccati equation," *Physical Chemistry Chemical Physics* **21**, 3761–3770 (2019).
- ¹²⁸R. Gutierrez, E. Díaz, R. Naaman, and G. Cuniberti, "Spin-selective transport through helical molecular systems," *Phys. Rev. B* **85**, 081404 (2012).
- ¹²⁹A.-M. Guo and Q.-f. Sun, "Spin-Selective Transport of Electrons in DNA Double Helix," *Phys. Rev. Lett.* **108**, 218102 (2012).
- ¹³⁰M. S. Zöllner, A. Saghatchi, V. Mujica, and C. Herrmann, "Influence of Electronic Structure Modeling and Junction Structure on First-Principles Chiral Induced Spin Selectivity," *J. Chem. Theory Comput.* **16**, 7357–7371 (2020).
- ¹³¹M. Cho, "Pure dephasing, quantum decoherence, and wave-particle duality," *Chem. Phys. Rev.* **4**, 021311 (2023).
- ¹³²A.-M. Guo and Q.-f. Sun, "Sequence-dependent spin-selective tunneling along double-stranded DNA," *Phys. Rev. B* **86**, 115441 (2012).
- ¹³³S. Matityahu, A. Aharonov, O. Entin-Wohlman, and C. A. Balseiro, "Spin filtering in all-electrical three-terminal interferometers," *Phys. Rev. B* **95**, 085411 (2017).
- ¹³⁴S. Varela, V. Mujica, and E. Medina, "Effective spin-orbit couplings in an analytical tight-binding model of DNA: Spin filtering and chiral spin transport," *Phys. Rev. B* **93**, 155436 (2016).
- ¹³⁵M. Geyer, R. Gutierrez, V. Mujica, and G. Cuniberti, "Chirality-Induced Spin Selectivity in a Coarse-Grained Tight-Binding Model for Helicene," *J. Phys. Chem. C* **123**, 27230–27241 (2019).
- ¹³⁶X. Li, J. Nan, and X. Pan, "Chiral induced spin selectivity as a spontaneous intertwined order," *Phys. Rev. Lett.* **125**, 263002 (2020).
- ¹³⁷J. Fransson, "Vibrational origin of exchange splitting and "chiral-induced spin selectivity," *Phys. Rev. B* **102**, 235416 (2020).
- ¹³⁸J. Fransson, "Charge Redistribution and Spin Polarization Driven by Correlation Induced Electron Exchange in Chiral Molecules," *Nano Lett.* **21**, 3026–3032 (2021).
- ¹³⁹C. Vittmann, J. Lim, D. Tamascelli, S. F. Huelga, and M. B. Plenio, "Spin-dependent momentum conservation of electron-phonon scattering in chirality-induced spin selectivity," *J. Phys. Chem. Lett.* **14**, 340–346 (2023).
- ¹⁴⁰H.-H. Teh, W. Dou, and J. E. Subotnik, "Spin polarization through a molecular junction based on nuclear Berry curvature effects," *Phys. Rev. B* **106**, 184302 (2022).
- ¹⁴¹A. G. Volosniev, H. Alpern, Y. Paltiel, O. Millo, M. Lemeshko, and A. Ghazaryan, "Interplay between friction and spin-orbit coupling as a source of spin polarization," *Phys. Rev. B* **104**, 024430 (2021).
- ¹⁴²L. Zhang, Y. Hao, W. Qin, S. Xie, and F. Qu, "Chiral-induced spin selectivity: A polaron transport model," *Phys. Rev. B* **102**, 214303 (2020).
- ¹⁴³J. Fransson, "Chirality-Induced Spin Selectivity: The Role of Electron Correlations," *J. Phys. Chem. Lett.* **10**, 7126–7132 (2019).
- ¹⁴⁴A. Dianat *et al.*, "Role of Exchange Interactions in the Magnetic Response and Intermolecular Recognition of Chiral Molecules," *Nano Lett.* **20**, 7077–7086 (2020).
- ¹⁴⁵Y. Kapon *et al.*, "Probing chiral discrimination in biological systems using atomic force microscopy: The role of van der Waals and exchange interactions," *J. Chem. Phys.* **159**, 224702 (2023).
- ¹⁴⁶S. Chen, R. Wu, and H.-H. Fu, "Persistent chirality-induced spin-selectivity effect in circular helix molecules," *Nano Lett.* **24**, 6210–6217 (2024).
- ¹⁴⁷W. Dednam *et al.*, "A group-theoretic approach to the origin of chirality-induced spin-selectivity in nonmagnetic molecular junctions," *ACS Nano* **17**, 6452–6465 (2023).
- ¹⁴⁸T.-R. Pan, A.-M. Guo, and Q.-F. Sun, "Effect of gate voltage on spin transport along \$alpha\$-helical protein," *Phys. Rev. B* **92**, 115418 (2015).
- ¹⁴⁹N. Sasao, H. Okada, Y. Utsumi, O. Entin-Wohlman, and A. Aharonov, "Spin-Current Induced Mechanical Torque in a Chiral Molecular Junction," *J. Phys. Soc. Jpn.* **88**, 064702 (2019).
- ¹⁵⁰J. Fransson and L. Turin, "Current induced spin-polarization in chiral molecules," *J. Phys. Chem. Lett.* **15**, 6370–6374 (2024).
- ¹⁵¹H. Chen *et al.*, "Chiral Phonon Diode Effect in Chiral Crystals," *Nano Lett.* **22**, 1688–1693 (2022).
- ¹⁵²T. Wang, H. Sun, X. Li, and L. Zhang, "Chiral phonons: Prediction, verification, and application," *Nano Lett.* **24**, 4311–4318 (2024).
- ¹⁵³C. Vittmann, R. K. Kassing, J. Lim, S. F. Huelga, and M. B. Plenio, "Interface-Induced Conservation of Momentum Leads to Chiral-Induced Spin Selectivity," *J. Phys. Chem. Lett.* **13**, 1791–1796 (2022).
- ¹⁵⁴A. López, S. Varela, and E. Medina, "Radiation modulated spin coupling in a double-stranded DNA model," *J. Phys.: Condens. Matter* **34**, 135301 (2022).
- ¹⁵⁵N. T. Phuc, "Floquet-engineered chiral-induced spin selectivity," *J. Chem. Phys.* **159**, 054706 (2023).
- ¹⁵⁶S. Chen and H.-H. Fu, "Chirality-induced majorana zero modes and majorana polarization," *ACS Nano* **18**, 34126–34133 (2024).
- ¹⁵⁷T.-Y. Zhang, Y. Mao, A.-M. Guo, and Q.-F. Sun, "Dynamical theory of chiral-induced spin selectivity in electron donor-chiral molecule-acceptor systems," *Phys. Rev. B* **111**, 205417 (2025).
- ¹⁵⁸S. Naskar, V. Mujica, and C. Herrmann, "Chiral-induced spin selectivity and non-equilibrium spin accumulation in molecules and interfaces: A first-principles study," *J. Phys. Chem. Lett.* **14**, 694–701 (2023).
- ¹⁵⁹S. S. Skourtis, D. N. Beratan, R. Naaman, A. Nitzan, and D. H. Waldeck, "Chiral Control of Electron Transmission through Molecules," *Phys. Rev. Lett.* **101**, 238103 (2008).
- ¹⁶⁰S. Alwan, A. Sharoni, and Y. Dubi, "Role of Electrode Polarization in the Electron Transport Chirality-Induced Spin-Selectivity Effect," *J. Phys. Chem. C* **128**, 6438–6445 (2024).
- ¹⁶¹N. Sukenik *et al.*, "Correlation between Ferromagnetic Layer Easy Axis and the Tilt Angle of Self Assembled Chiral Molecules," *Molecules* **25** (2020), 10.3390/molecules25246036.
- ¹⁶²A. Sharma *et al.*, "Control of magneto-optical properties of α -helical polyalanine self-assembled monolayers," *J. Mater. Chem. C* **8**, 11822–11829 (2020).
- ¹⁶³M. C. Hickey and J. S. Moodera, "Origin of intrinsic gilbert damping," *Phys. Rev. Lett.* **102**, 137601 (2009).
- ¹⁶⁴L. D. Barron, "False Chirality, Absolute Enantioselection and CP Violation: Pierre Curie's Legacy," *Magnetochemistry* **6** (2020), 10.3390/magnetochemistry6010005.
- ¹⁶⁵P. H. Alvarez, L. Gerhards, I. A. Solov'yov, and M. C. de Oliveira, "Quantum phenomena in biological systems," *Front. Quantum Sci. Technol. Volume 3 - 2024* (2024), 10.3389/fqst.2024.1466906.
- ¹⁶⁶L. Gerhards, A. Deser, D. R. Kattnig, J. Matysik, and I. A. Solov'yov, "Weak radiofrequency field effects on biological systems mediated through the radical pair mechanism," *Chem. Rev.* (2025), 10.1021/acs.chemrev.5c00178.
- ¹⁶⁷T. P. Fay, "Enantioselective radical reactions can be induced by electron spin polarization: A quantum mechanism for nature's emergent homochirality?" arXiv:2507.08287 (2025).
- ¹⁶⁸K. Michaeli, N. Kantor-Uziel, R. Naaman, and D. H. Waldeck, "The electron's spin and molecular chirality – how are they related and how do they affect life processes?" *Chem. Soc. Rev.* **45**, 6478–6487 (2016).
- ¹⁶⁹M. Geyer *et al.*, "The contribution of intermolecular spin interactions to the London dispersion forces between chiral molecules," *J. Chem. Phys.* **156**, 234106 (2022).
- ¹⁷⁰P. Hedegård, "Chiral-Induced Spin Selectivity in Capacitively Coupled Molecules," *J. Phys. Chem. A* **126**, 3157–3166 (2022).
- ¹⁷¹M. R. Safari, F. Matthes, C. M. Schneider, K.-H. Ernst, and D. E. Bürgler, "Spin-Selective Electron Transport Through Single Chiral Molecules," *Small* **20**, 2308233 (2024).
- ¹⁷²A. Nitzan, *Chemical Dynamics in Condensed Phases: Relaxation, Transfer and Reactions in Condensed Molecular Systems* (Oxford University Press, 2006).
- ¹⁷³V. May and O. Kühn, *Charge and energy transfer dynamics in molecular systems (3rd ed.)* (John Wiley & Sons, 2011).
- ¹⁷⁴A. Chiesa *et al.*, "Assessing the nature of chiral-induced spin selectivity by magnetic resonance," *J. Phys. Chem. Lett.* **12**, 6341–6347 (2021).

- ¹⁷⁵D. Kurzbach, D. R. Kattnig, B. Zhang, A. D. Schlüter, and D. Hinderberger, "Assessing the solution shape and size of charged dendronized polymers using double electron-electron resonance," *J. Phys. Chem. Lett.* **2**, 1583–1587 (2011).
- ¹⁷⁶D. R. Kattnig and D. Hinderberger, "Analytical distance distributions in systems of spherical symmetry with applications to double electron-electron resonance," *J. Magn. Reson.* **230**, 50–63 (2013).
- ¹⁷⁷E. Pyurbeeava, J. A. Mol, and P. Gehring, "Electronic measurements of entropy in meso- and nanoscale systems," *Chem. Phys. Rev.* **3**, 041308 (2022).
- ¹⁷⁸E. Pyurbeeava, C. Hsu, D. Vogel, C. Wegeberg, M. Mayor, H. van der Zant, J. A. Mol, and P. Gehring, "Controlling the entropy of a single-molecule junction," *Nano Lett.* **21**, 9715–9719 (2021).
- ¹⁷⁹J. Luo and P. J. Hore, "Chiral-induced spin selectivity in the formation and recombination of radical pairs: cryptochrome magnetoreception and EPR detection," *New J. Phys.* **23**, 043032 (2021).
- ¹⁸⁰Y. Tiwari and V. S. Poonia, "Quantum coherence enhancement by the chirality-induced spin selectivity effect in the radical-pair mechanism," *Phys. Rev. A* **107**, 052406 (2023).
- ¹⁸¹Y. Tiwari and V. S. Poonia, "Role of chiral-induced spin selectivity in the radical pair mechanism of avian magnetoreception," *Phys. Rev. E* **106**, 064409 (2022).
- ¹⁸²Y. Tiwari, P. Raghuvanshi, and V. S. Poonia, "Radical pair mechanism and the role of chirality-induced spin selectivity during planaria regeneration," *Appl. Phys. Lett.* **125**, 103701 (2024).
- ¹⁸³Y. Ren and P. J. Hore, "Conditions for epr detection of chirality-induced spin selectivity in spin-polarized radical pairs in isotropic solution," *J. Chem. Phys.* **159**, 145104 (2023).
- ¹⁸⁴T. P. Fay, "Chirality-Induced Spin Coherence in Electron Transfer Reactions," *J. Phys. Chem. Lett.* **12**, 1407–1412 (2021).
- ¹⁸⁵T. P. Fay and D. T. Limmer, "Origin of Chirality Induced Spin Selectivity in Photoinduced Electron Transfer," *Nano Lett.* **21**, 6696–6702 (2021).
- ¹⁸⁶P. B. Ayscough, P. J. Hore, C. G. Joslin, and K. A. McLauchlan, "Chemically induced dynamic electron polarization," in *Electron Spin Resonance*, Vol. 5, edited by P. B. Ayscough (The Royal Society of Chemistry, 1979).
- ¹⁸⁷T. P. Fay and D. T. Limmer, "Spin selective charge recombination in chiral donor-bridge-acceptor triads," *J. Chem. Phys.* **158**, 194101 (2023).
- ¹⁸⁸L. D. Smith, S. Tallapudi, M. C. Denton, and D. R. Kattnig, "Chirality-bolstered quantum zero effect enhances radical pair-based magnetoreception," arXiv:2505.01519 (2025).
- ¹⁸⁹M. R. Wasielewski, "Light-driven spin chemistry for quantum information science," *Physics Today* **76**, 28–34 (2023).
- ¹⁹⁰C.-Z. Wang, V. Mujica, and Y.-C. Lai, "Spin Fano Resonances in Chiral Molecules: An Alternative Mechanism for the CISS Effect and Experimental Implications," *Nano Lett.* **21**, 10423–10430 (2021).
- ¹⁹¹H. M. Hoang *et al.*, "Exciplexes versus loose ion pairs: How does the driving force impact the initial product ratio of photoinduced charge separation reactions?" *J. Phys. Chem. Lett.* **5**, 3188–3194 (2014).
- ¹⁹²Y. Wu and J. E. Subotnik, "Electronic spin separation induced by nuclear motion near conical intersections," *Nat. Commun.* **12**, 700 (2021).
- ¹⁹³S. S. Chandran, Y. Wu, H.-H. Teh, D. H. Waldeck, and J. E. Subotnik, "Electron transfer and spin-orbit coupling: Can nuclear motion lead to spin selective rates?" *J. Chem. Phys.* **156**, 174113 (2022).
- ¹⁹⁴N. Lambert, Y.-N. Chen, Y.-C. Cheng, C.-M. Li, G.-Y. Chen, and F. Nori, "Quantum biology," *Nat. Phys.* **9**, 10–18 (2013).
- ¹⁹⁵S. Firouzeh, M. A. Hossain, J. M. Cuerva, L. Álvarez de Cienfuegos, and S. Pramanik, "Chirality-induced spin selectivity in composite materials: A device perspective," *Acc. Chem. Res.* **57**, 1478–1487 (2024).
- ¹⁹⁶J. Lv, R. Sun, and X. Gao, "Emerging devices based on chiral nanomaterials," *Nanoscale* **17**, 3585–3599 (2025).
- ¹⁹⁷R. Naaman, Y. Paltiel, and D. H. Waldeck, "Chiral induced spin selectivity gives a new twist on spin-control in chemistry," *Acc. Chem. Res.* **53**, 2659–2667 (2020).
- ¹⁹⁸R. Naaman, Y. Paltiel, and D. H. Waldeck, "Chiral induced spin selectivity and its implications for biological functions," *Annu. Rev. Biophys.* **51**, 99–114 (2022).
- ¹⁹⁹M.-G. Kang *et al.*, "Room temperature chiral magnetoresistance in a chiral-perovskite-based perpendicular spin valve," *APL Materials* **12**, 081118 (2024).
- ²⁰⁰K. Kondou *et al.*, "Chirality-induced magnetoresistance due to thermally driven spin polarization," *J. Am. Chem. Soc.* **144**, 7302–7307 (2022).
- ²⁰¹A. C. Aragonès *et al.*, "Magnetoresistive single-molecule junctions: the role of the spinterface and the ciss effect," *Isr. J. Chem.* **62**, e202200090 (2022).
- ²⁰²K. H. Huisman and J. M. Thijssen, "Ciss effect: A magnetoresistance through inelastic scattering," *J. Phys. Chem. C* **125**, 23364–23369 (2021).
- ²⁰³S. H. Tirion and B. J. van Wees, "Hanle spin precession induced inverted magnetoresistance in chiral/semiconductor systems," *Appl. Phys. Lett.* **126**, 032402 (2025).
- ²⁰⁴B. Lim *et al.*, "Advances and key technologies in magnetoresistive sensors with high thermal stabilities and low field detectivities," *APL Materials* **10**, 051108 (2022).
- ²⁰⁵C. D. Bostick, S. Mukhopadhyay, I. Pecht, M. Sheves, D. Cahen, and D. Lederman, "Protein bioelectronics: a review of what we do and do not know," *Rep. Prog. Phys.* **81**, 026601 (2018).
- ²⁰⁶E. I. Latawiec *et al.*, "Detecting chirality-induced spin selectivity in chromophore-linked DNA hairpins using photogenerated radical pairs," *Proc. Natl. Acad. Sci.* **122**, e2515120122 (2025).
- ²⁰⁷Y. Zhang *et al.*, "Chirality detection of biological molecule through spin selectivity effect," *J. Chem. Phys.* **159**, 114703 (2023).
- ²⁰⁸P. K. Bhartiya, Suryansh, N. Bangruwa, M. Srivastava, and D. Mishra, "Light-amplified ciss-based hybrid qd-dna impedimetric device for DNA hybridization detection," *Anal. Chem.* **95**, 3656–3665 (2023).
- ²⁰⁹N. Bangruwa, Suryansh, M. Peralta, R. Gutierrez, G. Cuniberti, and D. Mishra, "Sequence-controlled chiral induced spin selectivity effect in ds-dna," *J. Chem. Phys.* **159**, 044702 (2023).
- ²¹⁰N. Bangruwa *et al.*, "Chiral-induced spin selectivity modulated time-correlated single-photon counting for DNA hybridization detection," *J. Phys. Chem. Lett.* **15**, 2384–2391 (2024).
- ²¹¹M. Tiwari and D. Mishra, "Enhanced spin-polarization and detection limit in a spin-based optoelectrochemical DNA hybridization sensor induced by circularly polarized light," *Sens. Diagn.* **3**, 1159–1166 (2024).
- ²¹²N. Bangruwa, M. Srivastava, and D. Mishra, "Ciss-based label-free novel electrochemical impedimetric detection of uvc-induced DNA damage," *ACS Omega* **7**, 37705–37713 (2022).
- ²¹³T. Georgiou *et al.*, "Enantiospecificity in nmr enabled by chirality-induced spin selectivity," *Nat. Commun.* **15** (2024), 10.1038/s41467-024-49966-8.
- ²¹⁴S. Mishra *et al.*, "Inducing circularly polarized single-photon emission via chiral-induced spin selectivity," *ACS Nano* **18**, 8663–8672 (2024).
- ²¹⁵J. Wang, B. Mao, and Z. V. Vardeny, "Chirality induced spin selectivity in chiral hybrid organic-inorganic perovskites," *J. Chem. Phys.* **159**, 091002 (2023).
- ²¹⁶D. R. Kattnig, B. Mladenova, G. Gramp, C. Kaiser, A. Heckmann, and C. Lambert, "Electron paramagnetic resonance spectroscopy of bis(triarylamine) paracyclophanes as model compounds for the intermolecular charge-transfer in solid state materials for optoelectronic applications," *J. Phys. Chem. C* **113**, 2983–2995 (2009).
- ²¹⁷M. D. Ventra, R. Gutierrez, and G. Cuniberti, "Chirality-induced spin-orbit coupling and spin selectivity," arXiv:2502.09338 (2025).
- ²¹⁸J. Dunlop, F. Cerisola, J. Tabanera-Bravo, and J. Anders, "Thermodynamically optimal protocols for dual-purpose qubit operations," *Phys. Rev. Res.* **6**, 033005 (2024).
- ²¹⁹T. Barron, "Mathematical models for therapeutic approaches involving electric conductors or shielding," arXiv:2505.20499 (2025).
- ²²⁰K. Wu and R. He, "Perspective: magnetic quantum sensors for biomedical applications," *Nanotechnology* **36**, 152501 (2025).
- ²²¹A. Lodesani, G. Anders, L. Bougas, T. Lins, D. Budker, P. Fierlinger, and C. D. Aiello, "Weak magnetic field effects in biology are measurable—accelerated xenopus embryogenesis in the absence of the geomagnetic field," *bioRxiv* (2024).
- ²²²A. Chiesa *et al.*, "Chirality-induced spin selectivity: An enabling technology for quantum applications," *Adv. Mater.* **35**, 2300472 (2023).
- ²²³S. Mishra, A. C. Jones, and C. Fontanesi, "Recent advancements in chiral spintronics: from molecular-level insights to device applications. a prospect based on the interplay between physical and chemical properties of chiral systems," *J. Mater. Chem. C* **13**, 2121–2134 (2025).
- ²²⁴F. Xie, H. Mao, C. Lin, Y. Feng, J. F. Stoddart, R. M. Young, and M. R. Wasielewski, "Quantum sensing of electric fields using spin-correlated radical ion pairs," *J. Am. Chem. Soc.* **145**, 14922–14931 (2023).

- ²²⁵C. L. Degen, F. Reinhard, and P. Cappellaro, “Quantum sensing,” *Rev. Mod. Phys.* **89**, 035002 (2017).
- ²²⁶S. I. Ilott, C. D. Pearse, B. Tigg, and D. R. Kattnig, “Electron hopping in cryptochromes: Implications for radical pair magnetoreception and the role of the fourth tryptophan,” *J. Chem. Phys.* **163**, 024110 (2025).
- ²²⁷F. Chowdhury, L. Smith, J. Glatthard, and D. Kattnig, “Probing the optimality of the radical pair quantum compass,” *Bull. Am. Phys. Soc.* (2024).
- ²²⁸H. G. Hiscock *et al.*, “Navigating at night: fundamental limits on the sensitivity of radical pair magnetoreception under dim light,” *Q. Rev. Biophys.* **52**, e9 (2019).
- ²²⁹J. N. Nelson, J. Zhang, J. Zhou, B. K. Rugg, M. D. Krzyaniak, and M. R. Wasielewski, “Effect of electron–nuclear hyperfine interactions on multiple-quantum coherences in photogenerated covalent radical (qubit) pairs,” *J. Phys. Chem. A* **122**, 9392–9402 (2018).
- ²³⁰C. Nielsen, D. R. Kattnig, E. Sjulstok, P. J. Hore, and I. A. Solov’ev, “Ascorbic acid may not be involved in cryptochromes-based magnetoreception,” *J. R. Soc. Interface* **14**, 20170657 (2017).
- ²³¹N. Lin and T. Mani, “Amplifying magnetic field effects on upconversion emission via molecular qubit-driven triplet-triplet annihilation,” *J. Am. Chem. Soc.* **147**, 7187–7190 (2025).
- ²³²Y. R. Poh and J. Yuen-Zhou, “Enhancing the optically detected magnetic resonance signal of organic molecular qubits,” *ACS Cent. Sci.* **11**, 116–126 (2025).
- ²³³P. J. Brown *et al.*, “Enhancing photogenerated radical pair properties in donor-chromophore-acceptor systems for quantum information applications,” *J. Phys. Chem. A* **128**, 9371–9382 (2024).
- ²³⁴S. M. Harvey and M. R. Wasielewski, “Photogenerated spin-correlated radical pairs: From photosynthetic energy transduction to quantum information science,” *J. Am. Chem. Soc.* **143**, 15508–15529 (2021).
- ²³⁵B. K. Rugg *et al.*, “Photodriven quantum teleportation of an electron spin state in a covalent donor–acceptor–radical system,” *Nat. Chem.* **11**, 981–986 (2019).
- ²³⁶P. H. Alvarez, F. T. Chowdhury, L. D. Smith, T. J. Brokowski, C. D. Aiello, D. R. Kattnig, and M. C. de Oliveira, “Simulating spin biology using a digital quantum computer: Prospects on a near-term quantum hardware emulator,” *APL Quantum* **1**, 036114 (2024).
- ²³⁷T. P. Fay, L. P. Lindoy, D. E. Manolopoulos, and P. J. Hore, “How quantum is radical pair magnetoreception?” *Faraday Discussions* **221**, 77–91 (2020).
- ²³⁸L. D. Smith, J. Deviers, and D. R. Kattnig, “Observations about utilitarian coherence in the avian compass,” *Sci. Rep.* **12**, 1–10 (2022).
- ²³⁹R. Jain, V. S. Poonia, K. Saha, D. Saha, and S. Ganguly, “The avian compass can be sensitive even without sustained electron spin coherence,” *Proc. R. Soc. A* **477**, 20200778 (2021).
- ²⁴⁰I. K. Kominis, “Quantum relative entropy shows singlet-triplet coherence is a resource in the radical-pair mechanism of biological magnetic sensing,” *Phys. Rev. Res.* **2**, 023206 (2020).
- ²⁴¹J. Cai and M. B. Plenio, “Chemical compass model for avian magnetoreception as a quantum coherent device,” *Phys. Rev. Lett.* **111**, 230503 (2013).
- ²⁴²E. M. Gauger, E. Rieper, J. J. L. Morton, S. C. Benjamin, and V. Vedral, “Sustained quantum coherence and entanglement in the avian compass,” *Phys. Rev. Lett.* **106**, 040503 (2011).
- ²⁴³I. K. Kominis and E. Gkoudinakis, “Approaching the quantum limit of energy resolution in animal magnetoreception,” *PRX Life* **3**, 013004 (2025).
- ²⁴⁴L. D. Smith, J. Glatthard, F. T. Chowdhury, and D. R. Kattnig, “On the optimality of the radical-pair quantum compass,” *Quantum Sci. Technol.* **9**, 035041 (2024).
- ²⁴⁵L. S. Guo, B. M. Xu, J. Zou, and B. Shao, “Quantifying magnetic sensitivity of radical pair based compass by quantum Fisher information,” *Sci. Rep.* **7**, 1–8 (2017).
- ²⁴⁶K. M. Vitalis and I. K. Kominis, “Quantum-limited biochemical magnetometers designed using the fisher information and quantum reaction control,” *Phys. Rev. A* **95**, 032129 (2017).
- ²⁴⁷A. Tateno, H. Nagashima, and K. Maeda, “Effect of frequency chirp on rydmer spectrum in awg-rydmer system at low magnetic field,” *Chem. Phys. Lett.* **864**, 141905 (2025).
- ²⁴⁸P. Hore, “Spin control of hybrid quantum-dot-based radical pairs,” *Nat. Mat.* , 1–2 (2025).
- ²⁴⁹F. T. Chowdhury, M. C. Denton, D. C. Bonser, and D. R. Kattnig, “Quantum control of radical-pair dynamics beyond time-local optimization,” *PRX Quantum* **5**, 020303 (2024).
- ²⁵⁰J. Cai, G. G. Guerreschi, and H. J. Briegel, “Quantum control and entanglement in a chemical compass,” *Phys. Rev. Lett.* **104**, 220502 (2010).
- ²⁵¹J. Luo, “Sensitivity enhancement of radical-pair magnetoreceptors as a result of spin decoherence,” *J. Chem. Phys.* **160**, 074306 (2024).
- ²⁵²D. R. Kattnig, J. K. Sowa, I. A. Solov’ev, and P. J. Hore, “Electron spin relaxation can enhance the performance of a cryptochrome-based magnetic compass sensor,” *New J. Phys.* **18**, 063007 (2016).
- ²⁵³L. D. Smith, F. T. Chowdhury, I. Peasgood, N. Dawkins, and D. R. Kattnig, “Driven radical motion enhances cryptochrome magnetoreception: Toward live quantum sensing,” *J. Phys. Chem. Lett.* **13**, 10500–10506 (2022).
- ²⁵⁴L. D. Smith, F. T. Chowdhury, J. Glatthard, and D. R. Kattnig, “Interradical motion can push magnetosensing precision towards quantum limits,” *arXiv:2506.21389* (2025).
- ²⁵⁵N. S. Babcock and D. R. Kattnig, “Radical scavenging could answer the challenge posed by electron–electron dipolar interactions in the cryptochrome compass model,” *JACS Au* **1**, 2033–2046 (2021).
- ²⁵⁶R. H. Keens, S. Bedekhal, and D. R. Kattnig, “Magnetsensitivity in dipolarly coupled three-spin systems,” *Phys. Rev. Lett.* **121**, 096001 (2018).
- ²⁵⁷D. R. Kattnig and P. J. Hore, “The sensitivity of a radical pair compass magnetoreceptor can be significantly amplified by radical scavengers,” *Sci. Rep.* **7**, 1–12 (2017).
- ²⁵⁸A. Dellis and I. Kominis, “The quantum zeno effect immunizes the avian compass against the deleterious effects of exchange and dipolar interactions,” *Biosystems* **107**, 153–157 (2012).
- ²⁵⁹I. K. Kominis, “Quantum Zeno effect explains magnetic-sensitive radical-ion-pair reactions,” *Phys. Rev. E* **80**, 056115 (2009).
- ²⁶⁰H. J. Eckvahl, G. Copley, R. M. Young, M. D. Krzyaniak, and M. R. Wasielewski, “Detecting chirality-induced spin selectivity in randomly oriented radical pairs photogenerated by hole transfer,” *J. Am. Chem. Soc.* **146**, 24125–24132 (2024).
- ²⁶¹K. Meng *et al.*, “Optically detected and radio wave-controlled spin chemistry in cryptochrome,” *arXiv:2504.16566* (2025), 10.48550/arXiv.2504.16566.
- ²⁶²M. P. Woods, “Quantum frequential computing: a quadratic run time advantage for all algorithms,” *arXiv:2403.02389* (2024).
- ²⁶³C.-J. Yu, S. von Kugelgen, D. W. Laorenza, and D. E. Freedman, “A molecular approach to quantum sensing,” *ACS Cent. Sci.* **7**, 712–723 (2021).
- ²⁶⁴N. Aslam, H. Zhou, E. K. Urbach, M. J. Turner, R. L. Walsworth, M. D. Lukin, and H. Park, “Quantum sensors for biomedical applications,” *Nat. Rev. Phys.* **5**, 157–169 (2023).
- ²⁶⁵M. Xie *et al.*, “Biocompatible surface functionalization architecture for a diamond quantum sensor,” *Proc. Natl. Acad. Sci.* **119**, e2114186119 (2022).
- ²⁶⁶S. Das, H. Mazumdar, K. R. Khondakar, Y. K. Mishra, and A. Kaushik, “Quantum biosensors: Principles and applications in medical diagnostics,” *ECS Sens. Plus* **3**, 025001 (2024).
- ²⁶⁷A. Finkler and D. Dasari, “Quantum sensing and control of spin-state dynamics in the radical-pair mechanism,” *Phys. Rev. Appl.* **15**, 034066 (2021).
- ²⁶⁸D. Khurana, R. H. Jensen, R. Giri, J. Bocquel, U. L. Andersen, K. Berg-Sørensen, and A. Huck, “Sensing of magnetic field effects in radical-pair reactions using a quantum sensor,” *Phys. Rev. Res.* **6**, 013218 (2024).
- ²⁶⁹W. Heisenberg, “Über quantentheoretische umdeutung kinematischer und mechanischer beziehungen,” *Z. Phys.* **33**, 879–893 (1925).
- ²⁷⁰G. E. Uhlenbeck and S. A. Goudsmit, “Ersetzung der hypothese vom unmechanischen zwang durch eineforderung bezüglich des inneren verhaltens jedes einzelnen elektrons,” *Naturwiss.* **13**, 953–954 (1925).